Journal of
Medicinal Chemistry

Article

Design, Synthesis, X-ray Crystallographic Analysis, and Biological Evaluation of Thiazole-Derivatives as Potent and Selective Inhibitors of Human Dihydroorotate Dehydrogenase

Junsheng Zhu, Le Han, Yanyan Diao, Xiaoli Ren, Minghao Xu, Liu-Xin Xu, shiliang li, Qiang Li, Dong Dong, Jin Huang, Xiaofeng Liu, zhenjiang zhao, Rui Wang, Lili Zhu, Yufang Xu, Xuhong Qian, and Honglin Li

J. Med. Chem., **Just Accepted Manuscript** • DOI: 10.1021/jm501127s • Publication Date (Web): 12 Jan 2015

Design, Synthesis, X-ray Crystallographic Analysis, and Biological Evaluation of Thiazole-Derivatives as Potent and Selective Inhibitors of Human Dihydroorotate Dehydrogenase

Junsheng Zhu[1,†], Le Han[1,2,†], Yanyan Diao[1,†], Xiaoli Ren[1], Minghao Xu[1], Liuxin Xu[1], Shiliang Li[1], Qiang Li[1], Dong Dong[1], Jin Huang[1], Xiaofeng Liu[1], Zhenjiang Zhao[1], Rui Wang[1], Lili Zhu[1,*], Yufang Xu[1], Xuhong Qian[2,*], Honglin Li[1,*]

[1] *State Key Laboratory of Bioreactor Engineering, Shanghai Key Laboratory of New Drug Design,* [2] *Shanghai Key Laboratory of Chemical Biology, School of Pharmacy, East China University of Science and Technology, Shanghai 200237, China.*

† Authors contributed equally to this work

* To whom correspondence should be addressed. Email: zhulfl@ecust.edu.cn, xhqian@ecust.edu.cn, hlli@ecust.edu.cn

Please address correspondence and requests for reprints to:

Prof. Honglin Li

School of Pharmacy, East China University of Science and Technology

130 Mei Long Road, Shanghai 200237

Phone/Fax: +86-21-64250213

Abstract. Human Dihydroorotate dehydrogenase (*Hs*DHODH) is a flavin-dependent mitochondrial enzyme, which has been certified as a potential therapeutic target for the treatment of rheumatoid arthritis and other autoimmune diseases. Based on lead compound **4,** which was previously identified as potential *Hs*DHODH inhibitor, a novel series of thiazole derivatives were designed and synthesized. The X-ray complex structures of the promising analogues **12** and **33** confirmed that these inhibitors bind at the putative ubiquinone binding tunnel and guided us to explore more potent inhibitors, such as compounds **44**, **46** and **47** which showed double digit nanomolar activities of 26 nM, 18 nM and 29 nM, respectively. Moreover, **44** presented considerable anti-inflammation effect in vivo and significantly alleviated foot swelling in a dose-dependent manner, which disclosed that thiazole-scaffold analogues can be possibly developed into the drug candidates for the treatment of rheumatoid arthritis by suppressing the bioactivity of *Hs*DHODH.

Keywords: Human dihydroorotate dehydrogenase (*Hs*DHODH), thiazole derivatives, structure-activity relationship (SAR).

Abbreviations: DHOase, dihydroorotase dihydroorotate; DHODH, dehydrogenase; *Hs*DHODH, Human dihydroorotate dehydrogenase; *Pf*DHODH, *Plasmodium falciparum* dihydroorotate dehydrogenase; DHO, dihydroorotate; ORO, Orotate; CoQ, ubiquinone; FMN, flavin mononucleotide; RA, rheumatoid arthritis; SAR, structure-activity relationship; CIA, collagen-induced arthritis.

Introduction

Pyrimidines serve essential functions in biosynthesis of DNA, RNA, and are linked by phosphodiester bridges to purine nucleotides in double-strand DNA.[1] Dihydroorotate dehydrogenase (DHODH), as the fourth enzyme of pyrimidine *de novo* synthesis, catalyzes the transformation of dihydroorotate (DHO) to orotate (ORO) with the participation of co-factors flavin mononucleotide (FMN) and ubiquinone (CoQ), representing the rate limiting step in pyrimidine biosynthesis.[2] DHODHs are divided into two classes in terms of cellular localization, amino acid sequence, and substrate/cofactor dependence.[3] Human dihydrooroate dehydrogenase (*Hs*DHODH) belongs to the family class 2 enzymes, characterized as a membrane-associated protein in eukaryotes that utilizes respiratory quinones as terminal electron acceptors,[4-6] which is unlike the family class 1 utilizing fumarate or NAD^+ in prokaryotes instead.[4, 5, 7] The location of *Hs*DHODH at the inner mitochondrial leaflet is functionally connected to the respiratory chain, ensuring the catalysis proceeds efficiently.

Generally, humans obtain pyrimidine by recycling existing ones in most cells, restricting the demand for the energetic *de novo* biosynthesis.[1] However, the gap between pyrimidine supply and demand in rapidly proliferating cells including tumor cells and the activated T-lymphocytes, B-lymphocytes, suggests their requirements on both *de novo* and salvage pathways.[8] The metabolism and multiplication modulated by DHODH determines it being a promising target for the development of new drug candidate.[2] The primary function of the mitochondrial electron transport chain further demonstrates the significance of developing new chemotherapeutic agents against *Hs*DHODH. Controlling *Hs*DHODH activities has been corroborated beneficial for the treatment of various diseases such as rheumatoid arthritis (RA), cancer and sclerosis.[9-11] Leflunomide (**1**) and brequinar (**3**) are two representative DHODH inhibitors (Figure 1). The former, a prodrug of its metabolite A771726 (**2**) (Figure 1), was implemented in treatment of RA in clinical trial.[8, 12-14] While the latter was initially applied in prevention of organ transplant rejection therapy and then regarded as antitumor and immunosuppressive agent in phase II clinical treatment.[15] However, the occurrence of severe side effects on both molecules limited their application. Long-term use of leflunomide would lead to reversible alopecia, hypertension, rash, diarrhea and abnormalities in liver enzymes.[14, 16-18] Oral administration of brequinar results in toxic effects when given in combination with cyclosporine or cis-platin.[19-21] Although exponential growth of researches was witnessed to explore the therapeutic potential of

*Hs*DHODH inhibitors in the past decades,[22-30] there are not successful cases reported yet with promising results in clinical trials.[2] As the therapeutic result, developing new chemotherapeutic agents targeting *Hs*DHODH remains a compelling therapeutic goal. We recently discovered several *Hs*DHODH inhibitors with different chemotypes by structure-based virtual screening, of which compound **4** (Figure 1) was selected as a promising structure for further optimization.[31] The initial structural modification of compound **4** produced compound **12** with the inhibitory activity improved by about 6 folds. The crystal complex structure of **12** and *Hs*DHODH was solved to confirm the putative binding poses of the thiazole-scaffold analogues in the ubiquinone binding tunnel, which led to further structure-based modification to improve the in vitro inhibitory activities. The most potent compounds achieved double-digit nanomolar activities and displayed the significance of anti-inflammation effect, suggesting their prospective roles as immunosuppressive and antiproliferative agents.

Results and Discussion

Chemistry

The synthesis route of compounds used in this study is shown in Scheme 1. Reaction of 3-chloropentane-2,4-dione or ethyl 2-chloro-3-oxobutanoate with derived thioureas, which were prepared in a facile three-step sequence using previously described methods,[32-34] gave **4-13** or **14-18** in good to excellent yields. Isothiocyanates were served as starting reactants to achieve compounds **19-20**, which also facilitated the synthesis of compounds **21-24** in alkaline conditions with the corresponding acyl chloride. Alternatively, to generate compounds **25-56**, we adopted one-pot strategies by the treatment of ethyl 3-cyclopropyl-3-oxopropanoate or ethyl 4,4-dimethyl-3-oxopentanoate or ethyl 3-oxo-3-phenylpropanoate with NBS in water in the presence of β-cyclodextrin, providing bromine-substituted β-keto esters as intermediates, which then undergo cyclization with substituted thioureas similarly as compounds **4-13** and **14-18**.

For compounds **49-53** and **54-56**, it was decided to synthesize the relevant aryl amine precursors **49c-53c**[35] and **54b-56b** (Schemes 2, 3). Compounds **49c-53c** were achieved under a palladium catalyzed cross-coupling reaction, which were conducted in a mixed solvent of water, ethanol and benzene, using appropriate phenylboronic acid, aniline, potassium carbonate and $Pd(PPh_3)_4$. Compounds **54b-56b** were provided via etherification, using proper aromatic substituted compounds and requisite aromatic alcohol or phenol under alkaline conditions in acetonitrile. Then the Fe-mediated reduction of nitro group to amino group was carried out in a solution of ammonium chloride and ethanol, which give the precursors **54b-56b**.

Preliminary Hydrophobic Group Modification on R^3

The lead compound **4** with a thiazole scaffold, a ubiquinone-binding competitive inhibitor of *Hs*DHODH, has recently been identified as a potential *Hs*DHODH inhibitor with an IC_{50} value of 3.937 μM (Table 1) through structure-based virtual screening in our previous work.[31] Compared with the reported DHODH inhibitors (Compounds **1-3**),[2,3,22-30] the compound **4** shared similar "thiazole moiety" as hydrogen bond-forming "head" linked via a nitrogen to an aromatic group as hydrophobic "tail".[3] According to the predicted binding pose in our previous work, the thiazole moiety of compound **4** located at the S2-S4 subsites tethered by several hydrogen bonds with the polar residues (Arg136, Gln47) in this hydrophilic region, and the 4-CH_3-3-Cl substituted phenyl ring then partially occupied the large hydrophobic region in S1 subsite,[31] which inspired us to increase the size and hydrophobicity of this moiety to occupy the rest of S1 subsite for leading improved inhibitory activity.

To identify more potent compounds, a systematic modification was performed by dividing the lead compound **4** into three fragments characterized by different pharmacophore features (Table 1): the sections of acetyl group (R^1), methyl group (R^2) and the aromatic motif (R^3, the referred "tail group"). Through the above analysis against the large hydrophobic S1 subsite, various substituents with some larger and more hydrophobic groups were introduced on R^3 as shown in Table 1. Unsubstituted or single *p*-position substituent (**5**, **6**, and **7**) did not show improved activities or deplete the activities comparing with lead compound **4**. Disubstituents at *p*- and *m*- position such as 3,4-di-CH_3 (**8**), 3-CF_3-4-Cl (**10**) and 3-CF_3-4-Br (**11**) showed a comparative potency to the original lead compound (**4**), as their R^3 section have similar hydrophobicity except 3-F-4-CH_3 (**9**) which knocked down the activity probably because of distinctive hydrophilic and electrostatic features of fluorine atom against other halogens. Augmenting the size and hydrophobicity of R^3 substituent with naphthyl moiety (**12**) significantly improved the inhibitory activity IC_{50} by almost 6 folds to 0.562 μM, rendering compound **12** as the most potent candidate against *Hs*DHODH identified in the preliminary SAR optimization attempt. However, the replacement of naphthyl **12** with anthracenyl **13** completely depleted the activity, suggesting the volume size of S1 subsite is limited and can not tolerate very bulky hydrophobic moieties.

Binding mode analysis through the crystal structure of *Hs*DHODH in complex with compound 12

In order to investigate the binding mode of the thiazole-based inhibitors, the most potent compound **12** so far was selected to co-crystallize with *Hs*DHODH. The structure was refined to 2.05 Å with excellent electron density (Table 2, Figure 2) and the coordinate of the complex structure had been deposited in the Protein Data Bank as the entry 4JGD. As shown in Figure 2A, *Hs*DHODH possesses a large C-terminal domain and a small N-terminal domain, linked by an extended loop. The large C-terminal harbors the redox site, where FMN and substrate dihydroorotate bind. On the other hand, The N-terminal extension consists of two helices *α*1 and *α*2, which features family class 2 enzymes.[3] A slot is formed between the two helices, within the short α1-α2 loop at the narrow end, contributing to the formation of a tunnel that ends at FMN cavity near the short α1-α2 loop. This tunnel narrows as it approaches to the proximal redox site. Previous study suggested ubiquinone probably inserted into the tunnel and thus easily approached FMN for the redox reaction.[6, 36-39] It is clearly noticed that the binding site of inhibitor **12** is formed between the two N-terminal helices, along with the reported inhibitors,[3, 40] again supporting the "putative ubiquinone tunnel" is a rational target for development of novel chemotherapeutics.

The solved structure showed in Figure 2B provided us further explanation for its potent activity. The binding site can be roughly divided into an exclusive hydrophobic entrance and a rather polar narrow end. The thiazole ring occupied the polar subsite in a planar conformation with the adjacent amide bond. There were totally two buried water molecules in the binding pocket: one formed a bridge between thiazole ring of the compound **12** and the guanidine group of Arg136, and the other one was hydrogen bonded to Gln47 and Thr360. Additionally, the carbonyl moiety on thiazole ring formed a direct hydrogen bond with Tyr356. The naththyl ring, occupied the bulky hydrophobic entrance as expected, exhibited several hydrophobic contacts with apolar residues like Met43, Leu46, Ala59, Phe62, Leu68, Phe98, Leu359 and Pro364, consisting with the fact that the entrance of the binding tunnel is almost made up by hydrophobic amino acids, as family class 2 enzymes are membrane associated.

Modification of R^1 Acyl group and R^2 methyl group

The co-crystal structure with **12** indicated that the inhibitor fits well in the binding region. But there was still some space for further modification to fit better in the binding site. For example, S4 subsite capped by Val134 and Val143 accessed to the proximal

FMN cofactor (Figure 3A) was near the R^1 position on compound **12**. This cavity can be presumably occupied by an alternative bulky group like an ethyl ester substituent. This hypothesis led to compounds **14-18** (Table 3) with maintained (**18** vs **12**) or improved inhibitory activities by 2-4 folds (**14** vs **6**, **15** vs **8**, **16** vs **9**, and **17** vs **4**). The results summarized above indicated that the ethyl ester group is easily accommodated with the inhibitor binding site herein and brings compounds closer to the FMN cofactor.

The impacts on R^2 from the size and polarity of the substituents were further assessed (Table 3). The replacement of -CH_3 with -NH_2 (compounds **19** and **20**) was strongly disfavored possibly because the occupied cavity is surrounded by the relatively hydrophobic environment involving side chains Pro52 and Val134 (Figure 3A). However, no improvement was achieved for the amide hydrophobic R^2 substituents, neither cyclopropane (**21** and **22**) nor phenyl (**23** and **24**). The unexpected activity loss may be caused by the formation of intramolecular hydrogen bond between the carbonyl oxygen of R^1 and the amide of R^2, which hindered the direct hydrogen bond to Tyr356. In contrast to the amide derivatives, the introduction of totally hydrophobic group at R^2 seemed to slightly improve the activities. The replacement by cyclopropyl (**25**, **26** and **27**) and tert-butyl (**28**, **29** and **30**) presented a 6 to 12-fold improvement in inhibitory activities compared with compound **4**. Interestingly, the phenyl substituents (**31**, **32** and **33**) significantly improved activity to double digit nanomolar level (IC_{50} = 58 nM, 49 nM, and 35 nM respectively).

To investigate the reason of the activities improvement for the phenyl substituents, compound **33** was selected to co-crystallize with *Hs*DHODH. The X-ray co-crystal structure of **33** with *Hs*DHODH (Figure 3A) indicated that when the size of R^2 is enlarged to the size of phenyl group, the "lower" side of subsite S4 is more suitable than the tiny "upper" hydrophobic pocket formed by Pro52 and Val143 to accommodate the larger phenyl moiety, and owing to the flexible characteristic of the amine linker, the binding mode of the thiazole moiety is shifted 180 degree compared with that of **12**. Specifically, the ethyl ester group of **33** formed hydrogen bond with Arg136 other than Tyr356, and the larger R^2 phenyl group was oriented toward Tyr356 and made close contact with Val134 and FMN. Considering that compound **33** displayed 100 folds more potency than lead **4**, it was concluded that the larger R^2 phenyl group induced binding style flip of thiazole moiety is beneficial for improving binding affinity, and the newly presented polar contacts in subsite S2 as well as the strengthened hydrophobic interactions in subsite S4 are key contributors for the potency boost that reached double digit nanomolar level.

Revisit R^3 modification for optimal hydrophobicity

23 new compounds were synthesized by coupling different amines moieties to the thiazole scaffold at R^3 in terms of various hydrophobicity and size to fine-tune the hydrophobicity effects on the activities, where R^1 was fixed as ethyl ester group and R^2 as phenyl group (Table 4). The inhibitory activity decreased sharply when the R^3 pheny group was unsubstituted (**34**) or only methoxyl substituted at *p*- position (**35**), indicating that the hydrophobic groups are exclusively favored at R^3. Consequently, the binding potency of the compounds in this round correlated well with their hydrophobicity except compound **36**, which showed similar activity to compounds **37** and **38** with chloride substitute. *p*- and *m*- disubstitutions yielded compounds **39-41** with sub-micromolar activities, while the 3,5-disubstitution (**42**) showed a slightly reduced inhibitory activity (**42** vs **41**). However, *o*- and *p*- disubstitution depleted activity completely (**43**), corresponding to the limited space of the narrow channel formed between aryl amine and thiazole ring as shown in figure 3A. We also evaluated the R^3 aromatic ring substituents' impacts on activities (Table 4). Compounds with fused bicyclic system R^3 substituents (**44-47**) showed improved activity especially for

compounds **44**, **46** and **47** (IC_{50} = 26 nM, 18 nM and 29 nM, respectively). The replacement of 5-indanyl (**44**) with 5-benzodioxolyl (**45**) reduced the activity (IC_{50} = 0.026 μM vs 1.108 μM, respectively), again corresponding to the hydrophobic nature of the binding cavity. Fused tricyclic substituents seemed unfavorable since compound **48** showed about 10-fold activity decrease comparing with compound **47**. However, almost all the biphenyl or biphenyl with additional linker system depleted inhibitory activity completely (compounds **49-52**, **54-56**), suggesting the steric constraints of the binding pocket in this area. These efforts on R^3 modification aforementioned led to remarkable improvement in inhibitory activity over those tested in the preliminary modification.

To thoroughly inspect the binding modes of the most potent compounds, a flexible docking study was performed for compound **47** based on the crystal structures reported in this study, using the Induced Fit Docking protocol in Maestro 9.0 (Schrödinger LLC). Just like the binding mode in the co-crystal structure of **33**, the carbanyl moiety of the ethyl ester group in **47** formed a hydrogen bond to Arg136 (Figure 3B) with the conformation of Met43 and Leu46 changed slightly to accommodate the ethyl ester group, while the phenyl fragment adopted a favorable configuration due to its well fitted size and hydrophobility with Pro52, Val134 andVal143. Meanwhile, the docking score of compound **47** was top-ranked (-10.17 kcal/mol), which is consistent with its inhibition activity (Table S1, Supporting Information). Moreover, by comparing the structures, binding modes and inhibition potencies of **12** and **47**, it was once again proved that the flip of thiazole moiety caused by the introduction of phenyl as R^2 in subsite S4 is favorable and the hydrogen bond between the R^1 ethyl ester group and Arg136 is also preferable for ameliorating binding affinity.

Species Selectivity Analysis of the Thiazole-Derivatives

Interestingly, compound **4** also presented a slightly inhibition potency against *pf*DHODH with an IC_{50} value of 0.630 μM.[31] To evaluate the species selectivity of the thiazole-derivatives, in vitro enzyme assay against *Plasmodium falciparum* dihydroorotate dehydrogenase (*Pf*DHODH) was performed (Tables 1, 3 and 4). One of the most potent compound **12** displayed comparable activities towards the two enzymes (IC_{50} = 0.562 μM vs 0.871 μM, respectively). In the preliminary optimization process, the hydrophobic group R^3 was modified and only two compounds (**7** and **11**) showed obvious selectivity over *Pf*DHODH. However, when larger substitutions were introduced to R^1 or R^2 group (**14-48**), the activities against *Pf*DHODH of almost all the compounds were totally lost. Remarkably, the inhibitors with larger volumes tend to exhibit preferential inhibition effects against *Hs*DHODH.

To further explore the structural basis of species selectivity of these thiazole-derivatives, the crystal structure of *Hs*DHODH in complex with compound **12** was aligned to reported *Pf*DHODH structure (PDB code: 3I65).[41] In *Pf*DHODH, residues Phe171 and Met536 were the corresponding residues Leu42 and Pro364 in *Hs*DHODH, respectively, which seal off the hydrophobic channel where the 3-chloro-4-methylphenyl group binds (Figure 4).[42] On the other hand, the substitutions of Ile263 for Val134 and Ile272 for Val143 made the R^2-occupied cavity smaller, which couldn't tolerate larger substituents such as tertiary butyl and phenyl groups. In conclusion, the species selectivity profile of these inhibitors was caused by the size constraints of the smaller *Pf*DHODH pocket, which was consistent with our previous study.[31, 43]

The initial thiazole-based lead compound **4** identified from virtual screening approach showed modest potency against *Hs*DHODH. In order to explore more and better potent inhibitors, a set of new derivatives were synthesized. The replacement of ethyl ester group on R^1 and phenyl group on R^2 led to the most potent series in our study. Naphthyl analogues (**44**, **46** and **47**) showed double digit nanomolar inhibitory activities against

*Hs*DHODH. By comparison of the more potent inhibitors with that displayed poor activity ones, we anticipated to obtain structural clues for future rational design study. First, the orientation of the thiazole moiety was largely influenced by the molecular size of hydrophobic groups at R^2 in subsite S4, which determines whether the polar substitute R^1 is hydrogen bonded to Arg136 in S2 or Tyr356 in S3. And a well-fitted phenyl group was recommended for R^2. As for R^1, some other polar groups like carbonyl and carboxyl were preferred to generate hydrogen bond in the hydrophilic region of S2 and S3. Then, the aromatic system on R^3 with two fused rings was favored. Aniline with mono bulky hydrophobic moiety at para position or combination of para and meta substitution were also well tolerated. Usually, the di-halogen substitutents on benzene were preferred. Additionally, the introduction at ortho postion on aniline should be avoidable since the binding site between thiazole and aryl amine is narrow. Finally, the sizable conformational change in S1 subsite may be paid more attention. Generally, it was the major factor to switch the selectivity between *Hs*DHODH and *Pf*DHODH.

Physicochemical Characterization

The physicochemical properties of all compounds were analyzed by Jaguar pKa prediction module,[44] XLOGP[45] and XLOGS[46] software. Selected inhibitors (**32**, **33**, **44**, and **47**) were also measured by Sirius T3 Station. The pKa values of the derivatives (**5-13**) varying between 0.5 and 2.3 were closely comparable to that of the hit compound **4** with predicted pKa at 1.6 (Table 1). The estimated logP showed variation between 3.25 and 5.75 where the logS of these derivatives (**5-13**) possessed values between -5.33 and -2.56 (Table 1). These values indicated that compunds **5-13** were low basic and shared poor solubility in water. The replacement of the acyl groups (R^1) with esters (compounds **14-18**) increase the pKa and logP values (**8** vs **15**, **12** vs **18**) albeit at a similar level of solubility. Modification on methyl group (R^2) with polar substituents such as amines, amides (**19-24**), and bulkiers (**25-30**) also did not improve solubility (Table 3). Finally, as discribed in table 4, compounds **34-56** bearing phenyl at R^2 and different hydrophobic substituents at R^3 reduced the pKa and logS whereas exhibited higher logP (**33** vs **17**, **47** vs **18**). All these calculated or measured molecular descriptors for these compounds will be used as the indicators for further optimizatation of the physicochemical and drug-like properties.

In vivo Anti-arthritic Effect of Compound 44

In this experiment, Wistar rats were treated with bovine type II collagen to induced arthritis (collagen - induced arthritis, CIA), then injected intraperitoneally with the compound **44** and methotrexate once per day for 28 days. The effect of compound **44** was evaluated by the arthritis swelling score and morphological observation of joint tissue of rats (Figure 5).

During experiment, control rats had shiny hair and normal eating. The body weight continuously increased, while the rats in model group showed a rough and dull hair, with a mild diarrhea at the beginning. The growth of body weight was markedly slower than that in normal group since day 9 (Figure 5A). Treatment of compound **44** and methotrexate had no obvious effect on the growth of body weight. Moreover, compound **44** displayed significant anti-arthritic efficacy in vivo ($p < 0.05$) and markedly alleviated foot swelling in a dose-dependent manner. Substantial anti-inflammation effects were be clearly observed after day 12 (both 5 mg/kg and 30 mg/kg, Figure 5B). After day 18, the arthritis scores in CIA rats reached to the peak and kept stable (Figure 5B). Compared to CIA rats, Methotrexate and compound **44** treated rats (in both dosage) significantly decreased the arthritis swelling score, indicated by obviously alleviated foot swelling in a dose related manner (Figures 5B and 5C). Moreover, hematoxylin and eosin (H&E) staining demonstrated that CIA rats exhibited histological changes of severe arthritis, showing substantial infiltration of inflammatory cells, synovial space exudation, synovial hyperplasia and cartilage erosion in joint tissues. Above-mentioned pathological features were markedly alleviated in rats treated with compound **44** in a dose-dependent manner (Figure 5D), indicating the significant of anti-inflammation effects. Briefly, the in vivo anti-arthritic effect of compound **44** were quite encouraging that it might serve as a promising lead compound for further development as immunosuppressant and antiproliferative agent targeting *Hs*DHODH.

Conclusion

We successfully identified a series of novel and promising thiazole-derivatives as inhibitors against *Hs*DHODH through structure-based lead optimization. Preliminary SAR deconvolution on lead compound **4** led to a potent compound **12,** then the crystal structures of the complex of *Hs*DHODH with compounds **12** and **33** were solved and analyzed to guide further SAR optimization aiming to increase the inhibitory activity. The SAR study reported here corresponds well to the structural analysis of the binding site and interaction modes observed from the crystal structure and leads to several promising compounds with double digit nanomolar activities, especially compounds **33**, **44**, **46** and **47** with IC_{50} values of 35nM, 26 nM, 18 nM, and 29 nM respectively, whereas their drug-like properties along with pharmacokinetic characteristics will be optimized further in the future work. Moreover, in vivo efficacy study demonstrated that compound **44** displayed considerable anti-arthritic effect and significantly alleviated foot swelling in a dose-dependent manner. In conjunction with the cocrystal structure data, these results further suggested that *Hs*DHODH is an effective target for rheumatoid arthritis chemotherapy and novel scaffolds designed in this work might lead to the discovery of new immunosuppressant and antiproliferative agents targeting *Hs*DHODH.

Experimental Section

In Vitro Enzyme Assay.

The pasmids coding for human and Plasmodium falciparum DHODH were kindly provided by Prof. Jon Clardy (Harvard Medical School). *Hs*DHODH (Met30-Arg396) and *Pf*DHODH (Phe158-Ser569) plasmid construction, protein expression and purification were followed the protocols of Liu and Deng respectively.[41, 47] The DHODH inhibition assays were carried out by using a DCIP assay method. The purified *Hs*DHODH was diluted into a final concentration of 10 nM with an assay buffer containing 50 mM HEPES pH 8.0, 150 mM KCl, then UQ_0 and DCIP were supplemented to the assay buffer to the final concentration of 100 μM and 120 μM respectively. For *Pf*DHODH, additional 0.1% triton X-100 was added.[48] The mixture was transferred into a 96-well plate and incubated for 5 min at room temperature. In the following step, the dihydroorotate was added to a final concentration of 500 μM to initiate the reaction. The reaction was monitored by measuring the decrease of DCIP in the absorption at 600 nm for each 30 s over a period of 6 min. Inhibition studies were performed in this assay with additional variable amounts of compounds. A771726 and DSM1 were also measured as the positive control for *Hs*DHODH and *Pf*DHODH respectively. Percent inhibition relative to the no inhibitor control was calculated from

$(1-V_i/V_0) \times 100\%$. For the determination of the IC_{50} values, 8-9 different concentrations were applied. Each inhibitor concentration point was tested in triplicate. IC_{50} values were calculated using the sigmoidal fitting option of the program Origin 8.0.

Co-crystallization of *Hs*DHODH with compounds 12 and 33

The complex crystals were cocrystallized by hanging-drop vapor diffusion method at 20 °C. Drops were formed on glass coverslips by mixing 1.5 μL of a 20 mg/mL protein solution in 50 mM HEPES pH 7.8, 400 mM NaCl, 30% glycerol, 1 mM EDTA, 10 mM N,N-dimethylundecylamin-N-oxide (C_{11}DAO), 2 mM dihydroorotate (DHO), and 1 mM compound **12** or **33** with an equal volume of precipitant solution consisting of 0.1 M acetate pH 4.8, 40 mM C_{11}DAO, 20.8 mM N,N-dimethyldecylamine-N-oxide (DDAO), 1.6-1.8 M ammonium sulfate. The drops were incubated against 1 mL of reservoir of 0.1 M acetate pH 4.8, 1.6-1.8 M ammonium sulfate and 30% glycerol. Crystals usually appeared as small yellow cubes within 3 days and reached a full size of $0.2\times0.2\times0.2$ mm^3 within 3 weeks.

Data Collection, Structure Determination, and Refinement.

X-ray diffraction data were collected at 100K at the synchrotron beamline BL17U1 of

SSRF (Shanghai, China). Statistics of data collection, processing, and refinement were summarized in Table 2. The data were processed with MOSFLM,[49] and scaled using the SCALA program from the CCP4 suite.[50] Structural elucidation and refinement were carried out using the CCP4 suite of programs.[50, 51] The crystal structure was determined by molecular replacement, using PDB entry 1D3G (without ligands and water molecules) as the template. REFMAC was employed for structure refinement.[52] The computer graphics program Coot,[53] implemented in the CCP4 suite, was used for interpretation of the electron density map and model building. The molecular graphics package PyMOL (DeLano, 2002) was used to generate the figures.

In vivo Efficacy Study.

Wistar rats (male, 130 ± 20 g), purchased from Shanghai SLRC Laboratory animal company, were housed in the condition of 20-25 °C, 50-60% relative humidity with a 12-hour light and night cycle. Food and water could be freely obtained. All procedures conform to the Chinese government guidelines for animal experiments. To establish CIA model, equal volume of bovine type II collagen (CII, Chondrex, USA) and incomplete Freund's adjuvant (IFA, Chondrex, USA) were emulsified using a high-speed homogenizer (IKA Co., Germany) on ice.[54] Compound **44** was freshly dissolved in a cosolvent consisted of 5% DMSO, 45% saline and 50% PEG200. 45 rats were randomly attributed into normal control (n = 9), CIA model (n = 8), Methotrexate treated group (n = 10) and 5 mg/kg (n = 10), 30 mg/kg (n = 8) compound **44** treated groups. Methotrexate, reported in the treatment of rheumatoid arthritis,[55] was used as positive control in present study.

At the beginning (day 0) of experiment, the rats were intradermally injected at the back base of the tail with 200 μL of the emulsified mixture containing 200 μg of CII. A booster injection of 100 μg CII was given at day 7 after primary immunization. Normal control received no treatment. The rats were injected intraperitoneally of compound **44** (5 mg/kg and 30 mg/kg) and Methotrexate (0.3 mg/kg), respectively, once per day for 28 days. At the meantime, the control group and model group were given the same amount of solvent.

During experiment, the weight of rats was recorded every three days. After the onset of arthritis, the foot swelling scores were recorded every two days under blinded conditions. The criteria of evaluation: 0 = no swelling; 1 = slight swelling; 2 = swelling; 3 = significant swelling; 4 = severe swelling. Since hind foot articular showed more pronounced swelling than forepaw, we used scoring criteria of maximum 8 points that was the total score of two hind feet to evaluate the incidence of rats' arthritis.

All rats were sacrificed after 28 day's treatment of compounds. Whole knee joints were fixed in 4% formalin for pathological detection. Tissue samples were decalcified in 10% EDTA for at least two weeks, then processed paraffin embedding, slice chopping and hematoxylin and eosin (H&E) staining. Stained sections were observed under optical microscope and photographed.

Data were expressed as mean ± standard error (mean ± SEM). SPSS statistical software was used to analyze the statistical significance of differences among groups, by one-way ANOVA following a multi-comparison analysis (LSD). $P \leqslant 0.05$ was considered to be statistically significant.[56]

Chemistry General Methods.

All chemical reagents and solvents were obtained from commercial sources and used without further purification. Thin-layer chromatography (TLC) was carried out to monitor the process of reactions. Purification of compounds was achieved by column chromatography with silica gel (Hailang, Qingdao) 200-300 mesh. ^1H NMR and ^{13}C NMR spectra were recorded on a Bruker AM-400 spectrometer with chemical shifts expressed as ppm (in $CDCl_3$, Me_4Si as internal standard). Melting points were analyzed on a WRS-1B-digital melting point apparatus. The mass spectra were measured at The Institute of Fine Chemistry of ECUST. Purity was determined using high-performance liquid chromatography spectrometry, which was operated on a Hewlett-Packard 1100 system chromatograph, equipping with Zorbax Eclipse XDB-C18 guard column (250 mm×4.6 mm) as an enrichment column. It adopted three methods descried as followed to check the purities. Method A: a gradient of 60-100% acetonitrile and 10 mM NH_4OAc in water (pH 6.0) (buffer) over 10 min at a flow rate of 1.0 mL/min. Method B: a gradient of 30-100% methanol and 10 mM NH_4OAc in water (pH 6.0) (buffer) over 20 minat a flow rate of 1.0 mL/min. Method C: a gradient of 30-100% acetonitrile and 10 mM NH_4OAc in water (pH 6.0) (buffer) over 10 min at a flow rate of 1.0 mL/min. Compounds synthesized in our laboratory were generally varied from 90% to 99% pure，the biological experiments were only employed on compounds whose purity is at least 95% pure.

*General Procedure for Compounds **4-56**.*These compounds were synthesized following the route described in Scheme 1 through intermediates **4a-18a, 35a-48a, 49d-53d, 54c-56c**.

*General Procedure for **4a-18a, 35a-48a, 49d-53d, 54c-56c**.*

A solution of substituted aniline (8.00 mmol) and triethylenediamine (24.00 mmol) in 10 mL acetone was stirred at ambient temperature for 10 min, after which 15 mL carbon disulphide was added dropwise. The resulting suspension was further stirred at room temperature overnight. Collecting the generating precipitate by filtration, washed by petroleum ether and dried at 70 °C for 6 h. The dried product was then dissolved in 20 mL chloroform, a solution of triphosgene (2.70 mmol) in 10 ml chloroform was added during 1 h, the reaction was continued to stir overnight and filtered to give a faint yellow solution, which was evaporated under vacuum, the concentrated substance was then purified by column chromatography using petroleum ether to afford the mediates **4a-18a, 35a-48a, 49d-53d, 54c-56c** with 50-70% yield.

*General Procedure for **4b-18b, 35b-48b, 49e-53e, 54d-56d**.*

A mixture of the corresponding isothiocyanates (5.00 mmol) and 1 mL ammonia water dissolved in 3 mL dichloromethane was stirred at 0 °C for 3 h. The resulting precipitate was filtered off and washed with petroleum ether. White solids were obtained in good yields.

*General Procedure for **4-18**.*

The appropriate thiourea (1.00 mmol) was added into a solution of 3-chloropentane-2,4-dione (1.00 mmol) or ethyl 2-chloro-3-oxobutanoate (1.00 mmol) and 20 mL methanol. The mixture was kept at refluxing overnight. After the corresponding solution cooling down to room temperature, 5% K_2CO_3 was used to neutralize it. Excess solvent was removed under vacuum. The crude product was extracted with ethyl acetate, which was then washed with brine, dried over Na_2SO_4 and concentrated in reduced pressure. The final product was achieved by further purification on column chromatography.

*General Procedure for **19** and **20**.*

Sodium ethylate (41 mmol) was carefully dissolved in ethanol (40 mL) at 0 ^{o}C. The resultant was added slowly into a mixture of cyanamide (41 mmol) and arylisothiocyanate (41 mmol) suspended in ethanol (25 mL). The solution was stirred overnight, followed by adding ethyl 2-chloroacetate (41 mmol), and the corresponding reactant was held for another 12 h at ambient temperature. Then the mixture was extracted with ethyl acetate, the organic layer was washed with brine, dried over Na_2SO_4 and concentrated in reduced pressure. The obtained crude product was further purified by column chromatography eluting with PE/EA (PE/EA=2/1, v/v) to give the target compound as white powder.

*General Procedure for **21-24**.*

Compounds **19** and **20** can be directly used as starting material for transformation. They were dissolved in 5 mL toluene and 15 drops of triethylamine were employed to provide an alkaline environment. The corresponding acyl chloride was added into the mixture dropwise over 10 minutes under ice-cooling. The reactant was then held at 90 ^{o}C until

TLC indicated the reaction was complete. After being cooled down to room temperature, extracted with ethyl acetate and collected the organic layer, followed by further purification using column chromatography with PE/EA (PE/EA=4/1, v/v), the final pure solid was achieved through further recrystallization.

General Procedure for ***25-56***.

β-cyclodextrin (0.50 mmol) was dissolved in 10 mL water, which would form a clear solution when the temperature reaches about 60 °C. Then a solution of ethyl 4,4-dimethyl-3-oxopentanoate, ethyl 3-cyclopropyl-3-oxopropanoate or ethyl benzoylacetate (0.50 mmol) in 0.5 mL acetone was added, followed by NBS (0.75 mmol). After stirring for 1 h at 60 °C, the appropriate thiourea (0.5 mmol) was added in one portion. The reaction was allowed to heat for 16-24 h, and then cooled down to room temperature, removal of the precipitate by filtration gave a yellowish solution, which was extracted with ethyl acetate, the organic layer was washed with brine, dried over Na_2SO_4 and concentrated in reduced pressure. The obtained crude product was further purified by column chromatography eluting with PE: EA mixtures, gradient from 8:1 to 5:1 to give the target compound as white or pale yellow powder.

General Procedure for ***49c-53c***.

To a stirred solution of 4-bromoaniline analogue (1.00 mmol) in 3 mL water, 3 mL ethanol and 10 mL benzene, appropriate phenylboronic acid (1.00 mmol) , potassium carbonate (10.00 mmol) were added, $Pd(PPh_3)_4$ (0.01 mmol) was added quickly while the mixture was at 80 ^oC under argon atmosphere, then the reaction was allowed to reflux overnight. Remove excess solvents under vacuum, the residue was extracted with dichloromethane and washed with brine. The combined organic layer was dried over Na_2SO_4 and concentrated to give a crude product that was further purified by column chromatography.

*General Procedure for **54a**.*

Phenol (40.00 mmol) was dissolved in 150 mL acetonitrile and potassium hydroxide flakes (50.00 mmol) was added. The mixture was warmed to 40 ^oC. A solution of 2-chloro-1-fluoro-4-nitrobenzene (40.00 mmol) in 60 mL acetonitrile was added, stirring was continued overnight at that temperature. Then cooled down the reaction to room temperature, which was then evaporated to remove excess solvent, the leaving residue was then extracted with ethyl acetate and brine. The combined organic layer was concentrated after drying over Na_2SO_4. The resulting crude was then purified by column chromatography using petroleum ether to afford yellow liquid as mediate **54a** with 95% yield.

*General Procedure for **55a**.*

Benzyl alcohol (40.00 mmol) was dissolved in 150 mL acetonitrile and potassium hydroxide flakes (50.00 mmol) was added. The mixture was warmed to 40 ^{o}C. A solution of 2-chloro-1-fluoro-4-nitrobenzene (40.00 mmol) in 60 mL acetonitrile was added, stirring was continued overnight at that temperature. Then cooled down the reaction to room temperature, quenched it with water. The resulting precipitate was filtered off and washed with water to afford yellow solid, which was used for the next step without purification.

General Procedure for ***56a***.

2-chloro-4-nitrophenol (7.61 mmol) was dissolved in 50 mL acetonitrile and potassium hydroxide flakes (9.51 mmol) was added. The mixture was warmed to 40 ^{o}C. A solution of 2-(bromomethyl)-1-chloro-3-fluorobenzene (7.61 mmol) in 20 mL acetonitrile was added, stirring was continued overnight at that temperature. Then cooled down the reaction to room temperature, quenched it with water. The resulting precipitate was filtered off and washed with water to afford yellow solid, which was used for the next step without purification.

General Procedure for ***54b-56b***.

A solution of ammonium chloride (48.40 mmol) in 10 mL water was added into a mixture of iron powder (16.13 mmol) and 25 mL ethanol. The appropriate nitro derivative (5.38 mmol) was added while the temperature reached 78 ^{o}C. The reaction was allowed to reflux for 0.5 h, cooled down to room temperature and then quenched by water. The resulting precipitate was filtered off and washed with water to afford the appropriate mediates, which was used for the next step without purification.

1-(2-((3-chloro-4-methylphenyl)amino)-4-methylthiazol-5-yl)ethanone (4). mp 197.3-198.0 ^{o}C. ^{1}H NMR (400MHz, DMSO-d_6): δ 10.79 (s, 1H), 7.80 (d, J = 2.0 Hz, 1H), 7.75 (dd, J_1= 2.4 Hz, J_2 = 8.4 Hz, 1H), 7.30 (d, J = 8.0 Hz, 1H), 2.55 (s, 3H), 2.42 (s, 3H), 2.27 (s, 3H). ^{13}C NMR (100 MHz, DMSO-d_6): δ 189.70, 165.12, 156.91, 139.58, 133.81, 131.93, 129.60, 123.15, 118.37, 117.12, 56.51, 30.17, 19.33, 19.00, 18.94. HRMS (ESI) calcd for: $C_{13}H_{13}ClN_2OS$ $[M+H]^+$ 281.0515, found 281.0515. Purity: 99.1% (method B, t_R = 14.38 min).

1-(4-methyl-2-(phenylamino)thiazol-5-yl)ethanone (5). mp 198.9-200.4 ^{o}C. ^{1}H NMR (400MHz, DMSO-d_6): δ 10.74 (s, 1H), 7.60 (d, J = 8.0 Hz, 2H), 7.37 (t, J = 8.0 Hz, 2H), 7.05 (t, J = 7.2 Hz, 1H), 2.56 (s, 3H), 2.43 (s, 3H). ^{13}C NMR (100 MHz, DMSO-d_6): 189.67, 165.69, 157.17, 140.41, 129.62, 123.28, 122.71, 118.62, 56.54, 30.12, 18.90. HRMS (ESI) calcd for: $C_{12}H_{12}N_2OS$ $[M+H]^+$ 233.0749, found 233.0746. Purity: 99.3% (method B, t_R = 9.94 min).

1-(2-((4-bromophenyl)amino)-4-methylthiazol-5-yl)ethanone (6). mp 209.9-210.7 °C. ^{1}H NMR (400MHz, DMSO-d_6): δ 10.87 (s, 1H), 7.61 (d, J = 8.8 Hz, 2H), 7.53 (d, J = 8.8 Hz, 2H), 2.56 (s, 3H), 2.44 (s, 3H). ^{13}C NMR (100 MHz, DMSO-d_6): 189.26, 164.55, 156.38, 139.30, 131.78, 122.76, 119.81, 113.93, 56.01, 29.68, 18.41. HRMS (ESI) calcd for: $C_{12}H_{11}BrN_2OS$ $[M+H]^+$ 310.9854, found 310.9854. Purity: 98.6% (method B, t_R = 13.52 min).

1-(2-((4-(tert-butyl)phenyl)amino)-4-methylthiazol-5-yl)ethanone (7). mp 174.1-174.8 °C. ^{1}H NMR (400MHz, DMSO-d_6): δ 10.68 (s, 1H), 7.49 (d, J = 8.4 Hz, 2H), 7.38 (d, J = 8.8 Hz, 2H), 2.54 (s, 3H), 2.42 (s, 3H), 1.28 (s, 9H). ^{13}C NMR (100 MHz, DMSO-d_6): 189.42, 165.92, 157.23, 145.81, 137.88, 126.29, 122.39, 118.59, 56.49, 34.51, 31.64, 30.16, 19.03, 18.93. HRMS (ESI) calcd for: $C_{16}H_{20}N_2OS$ $[M+H]^+$ 289.1375, found 289.1374. Purity: 96.1% (method B, t_R = 14.61 min).

1-(2-((3,4-dimethylphenyl)amino)-4-methylthiazol-5-yl)ethanone (8). mp 195.7-195.9 °C. ^{1}H NMR (400MHz, DMSO-d_6): δ 10.58 (s, 1H), 7.32 (d, J = 8.0 Hz, 1H), 7.28 (s, 1H), 7.11 (d, J = 8.4 Hz, 1H), 2.53 (s, 3H), 2.40 (s, 3H), 2.21 (s, 3H), 2.18 (s, 3H). ^{13}C

NMR (100 MHz, DMSO-d_6): δ 189.37, 166.12, 157.29, 138.21, 137.41, 131.42, 130.50, 122.25, 120.15, 116.41, 56.50, 30.12, 20.16, 19.22, 18.94. HRMS (ESI) calcd for: $C_{14}H_{16}N_2OS$ $[M+H]^+$ 261.1062, found 261.1065. Purity: 99.5% (method B, t_R = 12.41 min).

1-(2-((3-fluoro-4-methylphenyl)amino)-4-methylthiazol-5-yl)ethanone (9). mp 198.1-199.1°C. ^{1}H NMR (400MHz, DMSO-d_6): δ 10.81 (s, 1H), 7.60 (d, J = 12.0 Hz, 1H), 7.24-7.20 (m, 2H), 2.55 (s, 3H), 2.43 (s, 3H), 2.18 (s, 3H). ^{13}C NMR (100 MHz, DMSO-d_6): δ189.68, 165.14, 162.16, 159.77, 156.91, 139.84, 139.73, 132.23, 132.17, 123.10, 118.31, 118.14, 114.13, 114.11, 105.38, 105.11, 30.19, 18.93, 14.08, 14.06. HRMS (ESI) calcd for: $C_{13}H_{13}FN_2OS$ $[M+H]^+$ 265.0811, found 265.0807. Purity: 99.7% (method A, t_R = 5.82 min).

1-(2-((4-chloro-3-(trifluoromethyl)phenyl)amino)-4-methylthiazol-5-yl)ethanone (10). mp 231.1-231.6 °C. ^{1}H NMR (400MHz, DMSO-d_6): δ 11.13 (s, 1H), 8.26 (d, J = 2.4 Hz, 1H), 7.91 (dd, J_1= 2.4 Hz, J_2 = 8.8 Hz, 1H), 7.69 (d, J = 8.8 Hz, 1H), 2.58 (s, 3H), 2.46 (s, 3H). ^{13}C NMR (100 MHz, DMSO-d_6): 189.92, 164.46, 156.50, 139.80, 132.61, 127.51, 127.20, 124.49, 123.95, 123.03, 122.66, 121.77, 116.80, 116.74, 56.51, 30.11, 18.85. HRMS (ESI) calcd for: $C_{13}H_{10}ClF_3N_2OS$ $[M+H]^+$ 335.0233, found 335.0231. Purity: 98.7% (method B, t_R = 16.17 min).

1-(2-((4-bromo-3-(trifluoromethyl)phenyl)amino)-4-methylthiazol-5-yl)ethanone (11). mp 232.2-232.6 °C. ^{1}H NMR (400MHz, DMSO-d_6): δ 11.12 (s, 1H), 8.25 (s, 1H), 7.82 (s, 2H), 2.57 (s, 3H), 2.45 (s, 3H). ^{13}C NMR (100 MHz, DMSO-d_6): 189.95, 164.44, 156.51, 140.27, 136.01, 129.32, 129.01, 124.60, 124.00, 122.80, 121.88, 117.20, 117.14, 110.48, 56.51, 30.16, 18.88. HRMS (ESI) calcd for: $C_{13}H_{10}BrF_3N_2OS$ $[M+H]^+$ 378.9728, found 378.9724. Purity: 99.4% (method B, t_R = 16.48 min).

1-(4-methyl-2-(naphthalen-2-ylamino)thiazol-5-yl)ethan-1-one (12). mp 174.1-174.5 °C. ^{1}H NMR (400MHz, DMSO-d_6): δ 11.02 (s, 1H), 8.25 (d, J = 2.0 Hz, 1H), 7.91 (d, J = 8.8 Hz, 1H), 7.85 (d, J = 8.8 Hz, 2H), 7.61 (dd, J_1= 2.4 Hz, J_2 = 8.8 Hz, 1H), 7.51 – 7.47 (m, 1H), 7.43 – 7.39 (m, 1H), 2.62 (s, 3H), 2.46 (s, 3H). ^{13}C NMR (100 MHz, DMSO-d_6): 189.71, 165.44, 157.06, 138.10, 134.08, 129.86, 129.37, 128.02, 127.62, 127.15, 124.97, 123.03, 119.93, 113.72, 30.23, 19.01. HRMS (ESI) calcd for: $C_{16}H_{14}N_2OS$ $[M+H]^+$ 283.0905, found 283.0903. Purity: 95.2% (method B, t_R = 13.39 min).

1-(2-(anthracen-2-ylamino)-4-methylthiazol-5-yl)ethan-1-one (13). mp 232.8-233.8 °C. ^{1}H NMR (400MHz, DMSO-d_6): δ 11.06 (s, 1H), 8.51 – 8.47 (m, 3H), 8.10 – 8.04 (m, 3H), 7.57 – 7.45 (m, 3H), 2.65 (s, 3H), 2.48 (s, 3H). ^{13}C NMR (100 MHz, DMSO-d_6): 189.86, 165.15, 157.07, 137.37, 132.38, 132.18, 130.81, 129.86, 128.66, 128.56, 128.10, 126.45, 126.25, 125.40, 125.21, 123.30, 121.03, 112.01, 30.22, 18.98. HRMS (ESI) calcd for: $C_{20}H_{16}N_2OS$ $[M+H]^+$ 333.1062, found 333.1057. Purity: 95.4% (method B, t_R = 16.95 min).

Ethyl 2-((4-bromophenyl)amino)-4-methylthiazole-5-carboxylate (14). mp 189.7-190.1 °C. ^{1}H NMR (400MHz, DMSO-d_6): δ 7.62 (d, J = 8.8 Hz, 2H), 7.52 (d, J = 8.8 Hz, 2H), 4.22 (q, J = 7.2 Hz, 2H), 2.53 (s, 3H), 1.27 (t, J = 7.2 Hz, 3H). ^{13}C NMR (100 MHz, DMSO-d_6): 164.89, 162.26, 158.70, 139.96, 132.23, 120.23, 114.20, 109.97, 60.78, 17.78, 14.73. HRMS (ESI) calcd for: $C_{13}H_{13}BrN_2O_2S$ $[M+H]^+$ 340.9959, found 340.9951. Purity: 97.7% (method B, t_R = 17.56 min).

Ethyl 2-((3,4-dimethylphenyl)amino)-4-methylthiazole-5-carboxylate (15). mp 197.7-198.9 °C. ^{1}H NMR (400MHz, $CDCl_3$): δ 7.20-7.13 (m, 1H), 7.07 (d, J = 2.0 Hz, 2H), 4.27 (q, J = 7.2 Hz, 2H), 2.55 (s, 3H), 2.30 (s, 3H), 2.26 (s, 3H), 1.32 (t, J = 7.2 Hz, 3H). ^{13}C NMR (100 MHz, $CDCl_3$): δ 169.59, 162.67, 158.71, 138.14, 137.23, 133.86, 130.69, 122.80, 118.80, 60.47, 19.91, 19.26, 17.42, 14.44. HRMS (ESI) calcd for: $C_{15}H_{18}N_2O_2S$ $[M+H]^+$ 291.1167, found 291.1164. Purity: 98.2% (method B, t_R = 16.56 min).

Ethyl 2-((3-fluoro-4-methylphenyl)amino)-4-methylthiazole-5-carboxylate (16). mp 148.8-149.0 °C.^{1}H NMR (400MHz, DMSO-d_6): δ 10.73 (s, 1H), 7.60 (dd, J_1= 1.6 Hz, J_2= 12.2 Hz, 1H), 7.24 (t, J = 8.4 Hz, 1H), 7.19 (dd, J_1= 2.0 Hz, J_2= 8.4 Hz, 1H), 4.21 (q, J = 7.2 Hz, 2H), 2.53 (s, 3H), 2.18 (q, J = 1.2 Hz, 3H), 1.27 (t, J = 7.2 Hz, 3H).^{13}C NMR (100 MHz, $CDCl_3$) : δ167.80, 162.71, 162.49, 160.27, 158.48, 138.54, 138.43, 132.20, 132.14, 121.37, 121.20, 115.87, 115.83, 110.09, 107.73, 107.48, 60.68, 17.36, 14.41, 14.12, 14.09. HRMS (ESI) calcd for: $C_{14}H_{15}FN_2O_2S$ $[M+H]^+$ 295.0917, found 295.0916. Purity: 99.7% (method A, t_R = 8.14 min).

Ethyl 2-((3-chloro-4-methylphenyl)amino)-4-methylthiazole-5-carboxylate (17). mp 158.2-159.1 °C.^{1}H NMR (400MHz, DMSO-d_6): δ 7.82 (d, J = 2.0 Hz, 1H), 7.40 (dd, J_1= 2.0 Hz, J_2 = 8.4 Hz, 1H), 7.31 (d, J = 8.4 Hz, 1H), 4.22 (q, J = 7.2 Hz, 2H), 2.53 (s, 3H), 2.28 (s, 3H), 1.27 (t, J = 7.2 Hz, 3H). ^{13}C NMR (100 MHz, DMSO-d_6): 164.97, 162.26, 158.85, 139.71, 133.77, 131.93, 129.41, 118.29, 117.05, 109.86, 60.79, 19.33, 17.83, 14.74. HRMS (ESI) calcd for: $C_{14}H_{15}ClN_2O_2S$ $[M+H]^+$ 311.0621, found 311.0620. Purity: 95.3% (method B, t_R = 18.44 min).

Ethyl 4-methyl-2-(naphthalen-2-ylamino)thiazole-5-carboxylate (18). mp 163.1-164.0 ^{o}C. ^{1}H NMR (400MHz, CDCl$_3$): δ 7.90-7.84 (m, 4H), 7.54 (t, J = 7.6 Hz, 1H), 7.48 (t, J = 7.6 Hz, 1H),7.40 (dd, J_1= 2.4 Hz, J_2= 8.6 Hz, 1H),4.32 (q, J = 7.2 Hz, 2H), 2.61 (s, 3H), 1.37 (t, J = 7.2 Hz, 3H). ^{13}C NMR (100 MHz, CDCl$_3$): δ167.566, 162.482, 157.962, 136.648, 133.931, 130.779, 129.836, 127.789, 127.426, 127.031, 125.496, 120.362, 116.196, 109.969, 60.790, 17.313, 14.460. HRMS (ESI) calcd for: $C_{17}H_{16}N_2O_2S$ $[M+H]^+$ 313.1011, found 313.1012.Purity: 99.9% (method A, t_R = 9.01 min).

Ethyl 4-amino-2-((3,4-dimethylphenyl)amino)thiazole-5-carboxylate (19). mp 149.0-149.4 ^{o}C. ^{1}H NMR (400MHz, DMSO-d_6): δ 10.40 (s, 1H), 7.34 (d, J = 9.6 Hz, 1H), 7.31 (s, 1H), 7.09 (d, J = 8.4 Hz, 1H), 6.89 (s, 2H), 4.12 (q, J = 7.2 Hz, 2H), 2.21 (s, 3H), 2.18 (s, 3H), 1.21 (t, J = 7.2 Hz, 3H). ^{13}C NMR (100 MHz, DMSO-d_6): δ 166.06, 163.90, 138.14, 137.29, 131.40, 130.37, 120.46, 116.76, 59.30, 20.14, 19.22, 15.14. HRMS (ESI) calcd for: $C_{14}H_{17}N_3O_2S$ $[M+H]^+$ 292.1120, found 292.1117. Purity: 99.9% (method C, t_R = 9.57 min).

Ethyl 4-amino-2-((4-chloro-3-(trifluoromethyl)phenyl)amino)thiazole-5-carboxylate (20). mp 200.3-200.7 °C. ^{1}H NMR (400MHz, DMSO-d_6): δ 10.98 (s, 1H), 8.17 (d, J = 2.4 Hz, 1H), 7.92 (dd, J_1= 2.4 Hz, J_2= 8.8 Hz, 1H), 7.67 (d, J = 8.8 Hz, 1H), 6.98 (s, 2H), 4.15 (q, J = 7.2 Hz, 2H), 1.23 (t, J = 7.2 Hz, 3H). ^{13}C NMR (100 MHz, DMSO-d_6): δ 164.71, 163.86, 139.80, 132.68, 127.60, 127.29, 124.52, 123.22, 123.05, 121.80, 117.27, 117.22, 117.16, 117.10, 59.60, 15.09. HRMS (ESI) calcd for: $C_{13}H_{11}ClF_3N_3O_2S$ $[M+H]^+$ 366.0291, found 366.0292. Purity: 96.1% (method C, t_R = 7.10 min).

Ethyl 4-(cyclopropanecarboxamido)-2-((3,4-dimethylphenyl)amino)thiazole-5-carboxylate (21). mp 212.8-213.6 °C. ^{1}H NMR (400MHz, $CDCl_3$): δ 7.31 (d, J = 7.6 Hz, 1H), 7.13 (s,1H), 7.10 (d, J = 8.0 Hz, 1H), 5.62 (s, 1H), 4.27 (q, J = 7.2 Hz, 2H), 2.36 (s, 3H), 2.35 (s, 3H), 1.43-1.40 (m, 1H), 1.33 (t, J = 7.2 Hz, 3H), 1.20 – 1.18 (m, 2H), 0.84-0.81 (m, 2H). ^{13}C NMR (100 MHz, $CDCl_3$): δ 173.98, 165.07, 162.69, 159.21, 138.58, 138.17, 136.47, 130.99, 129.84, 126.20, 59.82, 19.93, 19.67, 14.53, 13.63, 10.62. HRMS (ESI) calcd for: $C_{18}H_{21}N_3O_3S$ $[M+H]^+$ 360.1382, found 360.1388. Purity: 97.0%

(method A, t_R = 7.61 min).

Ethyl 2-((4-chloro-3-(trifluoromethyl)phenyl)amino)-4-(cyclopropanecarboxamido)thiazole-5-carboxylate (22). mp 184.2-185.6 °C. ^{1}H NMR (400MHz, $CDCl_3$): δ 7.73-7.71 (m, 2H), 7.53 (dd, J_1= 2.0 Hz, J_2= 8.4 Hz, 1H), 4.28 (q, J = 7.20 Hz, 2H), 1.36-1.32 (m, 4H), 1.28-1.26 (m, 2H), 0.94-0.89 (m, 2H). ^{13}C NMR (100 MHz, $CDCl_3$): δ 172.82, 164.89, 161.82, 158.73, 137.63, 133.80, 133.46, 133.10, 130.27, 129.95, 128.81, 128.75, 128.70, 128.65, 123.50, 120.78, 60.07, 14.49, 13.98, 10.95. HRMS (ESI) calcd for: $C_{17}H_{15}ClF_3N_3O_3S$ $[M+H]^+$ 434.0553, found 434.0556. Purity: 99.2% (method A, t_R = 7.75 min).

Ethyl 4-benzamido-2-((3,4-dimethylphenyl)amino)thiazole-5-carboxylate (23). mp 203.1-205.2 °C. ^{1}H NMR (400MHz, $CDCl_3$): δ 7.31 (d, J = 8.0 Hz, 3H), 7.21 (t, J = 8.0 Hz, 2H), 7.09 (d, J = 8.0 Hz, 1H), 6.99 (s, 1H), 6.95 (d, J = 8.0 Hz, 1H), 5.67 (s, 2H), 4.31 (q, J = 7.2 Hz, 2H), 2.25 (s, 3H), 2.20 (s, 3H), 1.37 (t, J = 7.2 Hz, 3H). ^{13}C NMR (100 MHz, $CDCl_3$): δ 169.77, 165.03, 162.97, 159.19, 137.68, 137.43, 136.88. HRMS (ESI) calcd for: $C_{21}H_{21}N_3O_3S$ $[M+H]^+$ 396.1382, found 396.1381. Purity: 98.7% (method A, t_R = 7.51 min).

Ethyl 4-benzamido-2-((4-chloro-3-(trifluoromethyl)phenyl)amino)thiazole-5-carboxylate (24). mp 167.7-168.3 ^{o}C. ^{1}H NMR (400MHz, $CDCl_3$): δ 7.55 (d, J = 2.4 Hz, 1H), 7.48 (d, J = 8.8 Hz, 1H), 7.40-7.27 (m, 6H), 5.63 (s, 2H), 4.32 (q, J = 7.2 Hz, 2H), 1.38 (t, J = 7.2 Hz, 3H). ^{13}C NMR (100 MHz, $CDCl_3$): δ 169.13, 164.83, 161.83, 158.70, 138.11, 133.95, 133.26, 132.59, 132.23, 131.17, 129.39, 129.12, 129.07, 129.01, 128.96, 128.43, 128.34, 123.38, 120.66, 60.25, 14.55. HRMS (ESI) calcd for: $C_{20}H_{15}ClF_3N_3O_3S$ $[M+H]^+$ 470.0553, found 470.0554. Purity: 98.1% (method A, t_R = 8.06 min).

Ethyl 4-cyclopropyl-2-((3,4-dimethylphenyl)amino)thiazole-5-carboxylate (25). mp 145.4-145.7 ^{o}C. ^{1}H NMR (400MHz, $CDCl_3$): δ 7.52 (s, 1H), 7.14 (d, J = 8.8 Hz, 1H), 7.07 (d, J = 6.0 Hz, 2H), 4.32 (q, J = 7.2 Hz, 2H), 3.06 – 2.99 (m, 1H), 2.28 (s, 3H), 2.26 (s, 3H), 1.36 (t, J = 7.2 Hz, 3H), 1.10-1.09 (m, 2H), 1.04-1.02 (m, 2H). ^{13}C NMR (100 MHz, $CDCl_3$): δ 167.42, 164.91, 163.14, 137.98, 137.06, 132.92, 130.55, 121.13, 117.14, 108.84, 60.46, 19.95, 19.15, 14.50, 11.65, 9.75. HRMS (ESI) calcd for: $C_{17}H_{20}N_2O_2S$ $[M+H]^+$ 317.1324, found 317.1175. Purity: 99.4% (method A, t_R = 10.18 min).

Ethyl 4-cyclopropyl-2-((4-fluoro-3-methylphenyl)amino)thiazole-5-carboxylate (26). mp 181.2-183.3 °C. ^{1}H NMR (400 MHz, $CDCl_3$): δ 7.19-7.11 (m, 2H), 6.96 (dd, J_1 = 2.0 Hz, J_2 = 8.0 Hz, 1H), 4.33 (q, J = 7.2 Hz, 2H), 3.05-2.99 (m, 1H), 2.27 (s, 3H), 1.37 (t, J = 7.2 Hz, 3H), 1.11-1.09 (m, 2H), 1.07-1.04 (m, 2H). ^{13}C NMR (100 MHz, $CDCl_3$): δ 165.88, 164.58, 162.87, 162.65, 160.21, 138.35, 138.25, 132.04, 131.97, 120.46, 120.28, 114.35, 109.56, 106.36, 106.10, 60.61, 14.45, 14.03, 14.00, 11.63, 9.85. HRMS (ESI) calcd for: $C_{16}H_{17}FN_2O_2S$ $[M-H]^+$ 319.0917, found 319.0916. Purity: 99.2% (method A, t_R = 9.96 min).

Ethyl 2-((3-chloro-4-methylphenyl)amino)-4-cyclopropylthiazole-5-carboxylate (27). mp 188.0-188.7 °C. ^{1}H NMR (400MHz, $CDCl_3$): δ7.40 (d, J = 2.4 Hz, 1H), 7.22 (d, J = 8.4 Hz, 1H), 7.13 (dd, J_1 = 2.4 Hz, J_2 = 8.0 Hz, 1H), 4.33 (q, J = 7.2 Hz, 2H), 3.05 – 2.99 (m, 1H), 2.37 (s, 3H), 1.37 (t, J = 7.2 Hz, 3H), 1.13-1.09 (m, 2H), 1.07-1.03 (m, 2H). ^{13}C NMR (100 MHz, $CDCl_3$): δ 165.96, 164.67, 162.87, 138.04, 135.04, 131.76, 131.55, 119.73, 117.39, 60.60, 29.69, 19.39, 14.47, 11.63, 9.84. HRMS (ESI) calcd for: $C_{16}H_{17}ClN_2O_2S$ $[M+H]^+$ 337.0778, found 337.0770. Purity: 97.6% (method A, t_R = 11.22 min).

Ethyl 4-(tert-butyl)-2-((3,4-dimethylphenyl)amino)thiazole-5-carboxylate (28). mp

96.4-97.1 °C. ^1H NMR (400MHz, $CDCl_3$): δ 7.16 (d, J = 8.8 Hz, 1H), 7.10 (s, 2H), 4.28 (q, J = 7.2 Hz, 2H), 2.30 (s, 3H), 2.27 (s, 3H), 1.49 (s, 9H), 1.35 (t, J = 7.2 Hz, 3H). ^{13}C NMR (100 MHz, $CDCl_3$): δ 170.04, 165.38, 161.71, 138.05, 137.17, 132.74, 130.59, 120.84, 116.74, 109.63, 60.70, 36.39, 29.27, 20.02, 19.92, 19.20, 14.41. HRMS (ESI) calcd for: $C_{18}H_{24}N_2O_2S$ $[M+H]^+$ 333.1637, found 333.1633. Purity: 99.9% (method A, t_R = 12.16 min).

Ethyl 4-(tert-butyl)-2-((3-fluoro-4-methylphenyl)amino)thiazole-5-carboxylate (29). mp 75.2-75.7 °C. ^1H NMR (400MHz, $CDCl_3$): δ 7.20-7.15 (m, 2H), 6.99 (dd, J_1 = 2.0 Hz, J_2 = 8.0 Hz, 1H), 4.29 (q, J = 7.2 Hz, 2H), 2.28 (s, 3H), 1.50 (s, 9H), 1.37 (t, J = 7.2 Hz, 3H). ^{13}C NMR (100 MHz, $CDCl_3$): δ 169.59, 163.87, 162.69, 161.51, 160.25, 138.49, 138.38, 132.08, 132.01, 120.23, 120.05, 114.06, 114.03, 110.43, 106.05, 105.78, 60.90, 36.44, 29.26, 14.37. HRMS (ESI) calcd for: $C_{17}H_{21}FN_2O_2S$ $[M-H]^+$ 335.1230, found 335.1223. Purity: 99.2% (method A, t_R = 11.92 min).

Ethyl 4-(tert-butyl)-2-((3-chloro-4-methylphenyl)amino)thiazole-5-carboxylate (30). mp 85.0-87.0 °C. ^1H NMR (400MHz, $CDCl_3$): δ 7.47 (d, J = 2.0 Hz, 1H), 7.23 (d, J = 8.4 Hz, 1H), 7.16 (dd, J_1 = 2.4 Hz, J_2 = 8.4 Hz, 1H), 4.29 (q, J = 7.2 Hz, 2H), 2.37 (s, 3H), 1.49 (s, 9H), 1.36 (t, J = 7.2 Hz, 3H). ^{13}C NMR (100 MHz, $CDCl_3$): δ 169.80, 163.94, 161.58, 138.29, 135.03, 131.53, 131.40, 119.43, 117.06, 110.58, 60.87, 36.48, 29.29, 19.39, 14.36. HRMS (ESI) calcd for: $C_{17}H_{21}ClN_2O_2S$ $[M-H]^+$ 351.0934, found 351.0937. Purity: 99.9% (method A, t_R = 13.12 min).

Ethyl 2-((3,4-dimethylphenyl)amino)-4-phenylthiazole-5-carboxylate (31). mp 167.5-167.5 °C. ^{1}H NMR (400 MHz, $CDCl_3$): δ 7.74-7.72 (m, 2H), 7.40-7.39 (m, 3H), 7.12 (d, J = 8.4 Hz, 1H), 7.02 (dd, J_1 = 2.4 Hz, J_2 = 8.0 Hz, 1H), 6.97 (d, J = 2.0 Hz, 1H), 4.25-4.20 (m, 2H), 2.27 (s, 6H), 1.26 (t, J = 6.8 Hz, 3H). ^{13}C NMR (100 MHz, $CDCl_3$): δ 161.67, 158.13, 138.06, 136.90, 133.83, 133.63, 130.54, 129.73, 129.12, 127.67, 122.08, 122.02, 117.95, 117.90, 60.85, 19.93, 19.26, 14.24. HRMS (ESI) calcd for: $C_{20}H_{20}N_2O_2S$ $[M+H]^+$ 353.1324, found 353.1324. Purity: 95.6% (method A, t_R = 9.84 min).

Ethyl 2-((3-fluoro-4-methylphenyl)amino)-4-phenylthiazole-5-carboxylate (32). mp 156.3-156.8 °C. ^{1}H NMR (400MHz, $CDCl_3$): δ 7.72-7.70 (m, 2H), 7.38-7.37 (m, 3H), 7.08 (t, J = 7.6 Hz, 1H), 6.84-6.78 (m, 2H), 4.26-4.21 (m, 2H), 2.25 (s, 3H), 1.26 (t, J = 7.2 Hz, 3H). ^{13}C NMR (100 MHz, $CDCl_3$): δ 168.12, 162.43, 161.64, 159.99, 158.54, 138.48, 138.38, 133.99, 131.85, 131.79, 129.72, 129.12, 127.70, 121.08, 120.91, 115.66, 115.63, 110.09, 107.59, 107.33, 60.92, 29.73, 14.23, 14.12, 14.09. HRMS (ESI) calcd for: $C_{19}H_{17}FN_2O_2S$ $[M+H]^+$ 357.1073, found 357.1068. Purity: 95.1% (method A, t_R = 9.56 min).

Ethyl 2-((3-chloro-4-methylphenyl)amino)-4-phenylthiazole-5-carboxylate (33). mp 176.4-177.2 °C. ^{1}H NMR (400 MHz, $CDCl_3$): δ 7.74-7.72 (m, 2H), 7.40-7.39 (m, 3H), 7.23 (d, J = 2.4 Hz, 1H), 7.19 (d, J = 7.6 Hz, 1H), 7.03 (dd, J_1 = 2.4 Hz, J_2 = 8.0 Hz, 1H), 4.24 (q, J = 7.2 Hz, 2H), 2.37 (s, 3H), 1.27 (t, J = 7.2 Hz, 3H). ^{13}C NMR (100 MHz, $CDCl_3$): δ 167.73, 161.59, 158.47, 138.11, 134.93, 133.93, 132.44, 131.48, 129.66, 129.12, 127.69, 120.97, 118.66, 110.54, 60.92, 19.46, 14.21.HRMS (ESI) calcd for: $C_{19}H_{17}ClN_2O_2S$ $[M+H]^+$ 373.0778, found 373.0778. Purity: 96.6% (method A, t_R = 10.70 min).

Ethyl 4-phenyl-2-(phenylamino) thiazole-5-carboxylate (34). mp 176.2-177.0 °C. ^{1}H NMR (400 MHz, $CDCl_3$): δ 7.74-7.72 (m, 2H), 7.38 (d, J = 3.6 Hz, 3H), 7.38 (t, J = 8.0 Hz, 2H), 7.14 (d, J = 6.8 Hz, 3H), 4.26-4.21 (m, 2H), 1.26 (t, J = 6.8 Hz, 3H). ^{13}C NMR (100 MHz, $CDCl_3$): δ 178.42, 168.09, 161.76, 158.65, 139.35, 134.13, 129.79, 129.49, 129.14, 127.69, 124.47, 120.04, 109.92, 60.89, 29.58, 14.24.HRMS (ESI) calcd for: $C_{18}H_{16}N_2O_2S$ $[M+H]^+$ 325.1011, found 325.1009. Purity: 99.6% (method A, t_R = 7.96 min).

Ethyl 2-((4-methoxyphenyl)amino)-4-phenylthiazole-5-carboxylate (35). mp 133.4-133.7 °C. ^{1}H NMR (400 MHz, $CDCl_3$): δ 8.54 (s, 1H), 7.69 (dd, J_1 = 3.2 Hz, J_2 = 4.4 Hz, 2H), 7.37-7.35 (m, 3H), 7.14 (d, J = 9.2 Hz, 2H), 6.88 (d, J = 8.8 Hz, 2H), 4.20 (q, J = 7.2 Hz, 2H), 3.85 (s, 3H), 1.24 (t, J = 7.2 Hz, 3H). ^{13}C NMR (100 MHz, $CDCl_3$): δ 170.58, 161.75, 159.06, 157.30, 134.33, 132.62, 129.64, 128.87, 127.54, 123.84, 114.71, 109.40, 60.65, 55.51, 14.21. HRMS (ESI) calcd for: $C_{19}H_{18}N_2O_3S$ $[M+H]^+$ 355.1116, found 355.1115. Purity: 99.8% (method A, t_R = 7.54 min).

Ethyl 2-((4-chlorophenyl)amino)-4-phenylthiazole-5-carboxylate (36). mp 154.3-156.2 °C. ^{1}H NMR (400MHz, $CDCl_3$): δ 10.59 (s, 1H), 7.67 (d, J = 6.4 Hz, 2H), 7.36-7.28 (m, 3H), 7.13 (d, J = 8.4 Hz, 2H), 6.85 (d, J = 8.8 Hz, 2H), 4.25-4.20 (m, 2H), 1.25 (t, J = 7.2 Hz, 3H). ^{13}C NMR (100 MHz, $CDCl_3$): δ 168.23, 161.60, 158.519, 137.94, 134.03, 129.76, 129.59, 129.41, 129.23, 127.74, 121.57, 110.14, 60.98, 14.22. HRMS (ESI) calcd for: $C_{18}H_{15}ClN_2O_2S$ $[M+H]^+$ 359.0621, found 359.0615. Purity: 99.0% (method A, t_R = 9.69 min).

Ethyl 4-phenyl-2-((4-(trifluoromethyl)phenyl)amino)thiazole-5-carboxylate (37). mp 189.6-190.8 °C. ^{1}H NMR (400MHz, $CDCl_3$): 7.78-7.75 (m, 2H), 7.59 (d, J = 8.4 Hz, 2H), 7.43-7.41 (m, 3H), 7.34 (d, J = 8.4 Hz, 2H), 4.30-4.25 (m, 2H), 1.29 (t, J = 7.2 Hz, 3H).

^{13}C NMR (100 MHz, $CDCl_3$): δ 166.39, 161.50, 158.21, 142.18, 133.82, 129.81, 129.43, 127.79, 126.62, 126.59, 118.66, 111.10, 61.17, 14.21. HRMS (ESI) calcd for: $C_{19}H_{15}F_3N_2O_2S$ $[M+H]^+$ 393.0885, found 393.0884. Purity: 99.0% (method A, t_R = 9.86 min).

Ethyl 2-((4-(tert-butyl)phenyl)amino)-4-phenylthiazole-5-carboxylate (38). mp 161.3-163.3 °C. ^1H NMR (400MHz, $CDCl_3$): δ 7.75-7.73 (m, 2H), 7.40-7.38 (m, 5H), 7.19 (d, J = 8.4 Hz, 2H), 4.26-4.21 (m, 2H), 1.36 (s, 9H), 1.27 (t, J = 7.2 Hz, 3H). ^{13}C NMR (100 MHz, $CDCl_3$): δ 168.40, 161.72, 158.73, 147.77, 136.66, 134.20, 129.73, 129.01, 127.56, 126.35, 120.19, 109.85, 60.75, 34.43, 31.34, 14.24. HRMS (ESI) calcd for: $C_{22}H_{24}N_2O_2S$ $[M+H]^+$ 381.1637, found 381.1635. Purity: 99.1% (method B, t_R = 21.11 min).

Ethyl 2-((4-chloro-3-(trifluoromethyl)phenyl)amino)-4-phenylthiazole-5-carboxylate (39). mp 161.7-162.3 °C. ^1H NMR (400MHz, $CDCl_3$): δ 7.70-7.67 (m, 2H), 7.50 (d, J = 2.8 Hz, 1H), 7.38-7.32 (m, 4H), 7.22 (dd, J_1= 2.8 Hz, J_2= 8.8 Hz, 1H), 4.28-4.23 (m, 2H), 1.27 (t, J = 7.2 Hz, 3H). ^{13}C NMR (100 MHz, $CDCl_3$): δ 166.90, 161.48, 158.24, 138.21, 133.55, 132.36, 129.68, 129.36, 127.74, 126.95, 123.85, 120.96, 119.02, 118.97, 111.14, 61.22, 14.18. HRMS (ESI) calcd for: $C_{19}H_{14}ClF_3N_2O_2S$ $[M+H]^+$ 427.0495, found 427.0493. Purity: 96.3% (method A, t_R = 11.06 min).

Ethyl 2-((4-bromo-3-(trifluoromethyl)phenyl)amino)-4-phenylthiazole-5-carboxylate (40). mp 154.1-154.3 °C. ^{1}H NMR (400MHz, $CDCl_3$): δ 7.69-7.67 (m, 2H), 7.53 (d, J = 8.8 Hz, 1H), 7.47 (d, J = 2.8 Hz, 1H), 7.33-7.29 (m, 3H), 7.10 (dd, J_1= 2.8 Hz, J_2= 8.6 Hz, 1H), 4.28-4.23 (m, 2H), 1.28 (t, J = 7.2 Hz, 3H). ^{13}C NMR (100 MHz, $CDCl_3$): δ 166.75, 161.45, 158.13, 138.81, 135.82, 133.48, 129.68, 129.37, 127.74, 123.77, 119.19, 119.13, 113.92, 111.25, 61.22, 14.15. HRMS (ESI) calcd for: $C_{19}H_{14}BrF_3N_2O_2S$ $[M+H]^+$ 470.9990, found 470.9986. Purity: 97.8% (method A, t_R = 11.33 min).

Ethyl 2-((3,4-dichlorophenyl)amino)-4-phenylthiazole-5-carboxylate (41). mp 155.2-155.6 °C. ^{1}H NMR (400MHz, $CDCl_3$): δ 7.70-7.67 (m, 2H), 7.35 (dd, J_1= 2.0 Hz, J_2= 5.4 Hz, 3H), 7.26 (d, J = 8.8 Hz, 1H), 7.14 (d, J = 2.4 Hz, 1H), 6.88 (dd, J_1= 2.8 Hz, J_2= 8.6 Hz, 1H), 4.27-4.22 (m, 2H), 1.27 (t, J = 7.2 Hz, 3H). ^{13}C NMR (100 MHz, $CDCl_3$): δ 167.54, 161.52, 158.29, 138.82, 133.68, 133.09, 130.82, 129.65, 129.34, 127.83, 127.76, 121.83, 119.38, 110.73, 61.14, 14.22. HRMS (ESI) calcd for: $C_{18}H_{14}Cl_2N_2O_2S$ $[M+H]^+$ 393.0231, found 393.0234. Purity: 95.4% (method A, t_R = 11.11 min).

Ethyl 2-((3,5-dichlorophenyl)amino)-4-phenylthiazole-5-carboxylate (42). mp98.6-99.1 °C. ^{1}H NMR (400MHz, $CDCl_3$): δ 7.74-7.72 (m, 2H), 7.39-7.37 (m, 3H), 7.06 (d, J = 1.6 Hz, 1H), 7.00 (d, J = 1.6 Hz, 2H), 4.30-4.24 (m, 2H), 1.29 (t, J = 7.2 Hz, 3H). ^{13}C NMR (100 MHz, $CDCl_3$): δ 166.16, 161.45, 158.13, 141.13, 135.68, 133.54, 129.65, 129.44, 127.87, 124.12, 117.67, 111.64, 61.20, 14.20. HRMS (ESI) calcd for: $C_{18}H_{14}Cl_2N_2O_2S$ $[M+H]^+$ 393.0231, found 393.0231. Purity: 98.2% (method A, t_R = 11.83 min).

Ethyl 2-((4-bromo-2-methylphenyl)amino)-4-phenylthiazole-5-carboxylate (43). mp 171.4-173.3 °C.^{1}H NMR (400MHz, $CDCl_3$): δ 7.52-7.50 (m, 2H), 7.36 (dd, J_1= 2.4 Hz, J_2= 8.4 Hz, 1H), 7.29 (d, J = 2.0 Hz, 1H), 7.27-7.23 (m, 2H), 7.15 (t, J = 3.6 Hz, 2H), 4.19-4.14 (m, 2H), 2.08 (s, 3H), 1.21 (t, J = 7.2 Hz, 3H). ^{13}C NMR (100 MHz, $CDCl_3$): δ 170.40, 161.54, 158.93, 137.12, 135.76, 134.12, 133.79, 130.28, 129.26, 128.90, 127.39, 126.33, 126.29, 120.14, 110.18, 60.80, 29.73, 17.45, 14.19. HRMS (ESI) calcd for: $C_{19}H_{17}BrN_2O_2S$ $[M+H]^+$ 417.0272, found 417.0271. Purity: 95.2% (method A, t_R = 10.27 min).

Ethyl 2-((2,3-dihydro-1H-inden-5-yl)amino)-4-phenylthiazole-5-carboxylate (44). mp 163.2-164.1 °C. ^{1}H NMR (400MHz, $CDCl_3$): δ 7.74-7.73 (m, 2H), 7.39-7.38 (m, 3H), 7.19 (d, J = 8.0 Hz, 1H), 7.07-6.99 (m, 2H), 4.25-4.20 (m, 2H), 2.91 (t, J = 7.6 Hz, 4H), 2.14-2.07 (m, 2H), 1.26 (t, J = 7.2 Hz, 3H). ^{13}C NMR (100 MHz, $CDCl_3$): 161.78, 158.78, 145.92, 141.21, 137.52, 134.27, 129.73, 128.96, 127.62, 125.07, 118.72, 117.07, 117.03, 60.75, 33.01, 32.38, 25.63, 14.25. HRMS (ESI) calcd for: $C_{21}H_{20}N_2O_2S$ $[M+H]^+$ 365.1324, found 365.1326. Purity: 96.2% (method A, t_R = 10.42 min).

Ethyl 2-(benzo[d][1,3]dioxol-5-ylamino)-4-phenylthiazole-5-carboxylate (45). mp 125.6- 126.4 °C. ^{1}H NMR (400MHz, $CDCl_3$): δ 7.68-7.66 (m, 2H), 7.37-7.34 (m, 3H), 6.75 (d, J = 8.0 Hz, 1H), 6.65-6.68 (m, 2H), 6.01 (s, 2H), 4.23-4.18 (m, 2H), 1.24 (t, J = 7.2 Hz, 3H). ^{13}C NMR (100 MHz, $CDCl_3$): δ 170.08, 161.65, 158.74, 148.25, 145.35, 134.03, 133.70, 130.02, 129.61, 128.93, 128.25, 127.57, 115.41, 109.67, 108.51, 104.05, 101.51, 60.75, 14.20. HRMS (ESI) calcd for: $C_{19}H_{16}N_2O_4S$ $[M+H]^+$ 369.0909, found 369.0902. Purity: 99.5% (method A, t_R = 7.28 min).

Ethyl 4-phenyl-2-((5,6,7,8-tetrahydronaphthalen-2-yl)amino)thiazole-5-carboxylate (46). mp 156.2-156.5 °C. ^{1}H NMR (400MHz, $CDCl_3$): δ 7.76-7.73 (m, 2H), 7.42-7.41 (m, 3H), 7.72 (d, J = 8.4 Hz, 1H), 7.02 (dd, J_1= 2.4 Hz, J_2= 7.4 Hz, 1H), 6.94 (d, J = 2.0 Hz, 1H), 4.27-4.21 (m, 2H), 2.78 (s, 4H), 1.85-1.81 (m, 4H), 1.26 (t, J = 7.2 Hz, 3H). ^{13}C NMR (100 MHz, $CDCl_3$): δ 168.61, 161.77, 158.71, 138.50, 136.68, 134.24, 134.14, 130.06, 129.74, 128.94, 127.58, 121.17, 118.02, 109.86, 60.72, 29.46, 28.95, 23.15, 22.98, 14.24. HRMS (ESI) calcd for: $C_{22}H_{22}N_2O_2S$ $[M+H]^+$ 379.1480, found 379.1481. Purity: 99.5% (method A, t_R = 11.36 min).

Ethyl 2-(naphthalen-2-ylamino)-4-phenylthiazole-5-carboxylate (47). ^{1}H NMR (400MHz, DMSO-d_6): δ 10.90 (s, 1H), 8.23 (s, 1H), 7.92-7.63 (m, 6H), 7.52-7.34 (m, 5H), 4.27 (q, J = 7.2 Hz, 2H), 1.30 (t, J = 7.2 Hz, 3H). ESI $[M+H]^+$ found 375.3. Purity: 95.2%.

Ethyl 2-(anthracen-2-ylamino)-4-phenylthiazole-5-carboxylate (48). mp 229.2-229.6 ^{o}C.^{1}H NMR (400MHz, $CDCl_3$): 8.43 (s, 2H), 8.03 (d, J = 8.8 Hz, 3H), 7.99 (d, J = 2.0 Hz, 1H), 7.83-7.81 (m, 2H), 7.54-7.46 (m, 5H), 7.27 (d, J = 2.0 Hz, 1H), 4.32-4.27 (m, 2H), 1.31 (t, J = 7.2 Hz, 3H). ^{13}C NMR (100 MHz, $CDCl_3$): δ 165.74, 161.57, 135.64, 133.72, 132.47, 131.68, 131.33, 130.35, 129.81, 129.39, 128.98, 128.27, 127.88, 127.82, 126.44, 126.00, 125.45, 125.32, 120.37, 113.57, 111.20, 61.11, 14.27, HRMS (ESI) calcd for: $C_{26}H_{20}N_2O_2S$ $[M+H]^+$ 425.1324, found 425.1324. Purity: 98.6% (method A, t_R = 12.09 min).

Ethyl 2-([1,1'-biphenyl]-4-ylamino)-4-phenylthiazole-5-carboxylate (49). mp

154.8-157.3 °C. ^{1}H NMR (400MHz, $CDCl_3$): δ 8.11-8.09 (m, 1H), 7.76-7.74 (m, 2H), 7.64-7.61 (m, 4H), 7.48-7.44 (m, 5H), 7.38 (d, J = 8.0 Hz, 2H), 4.26 (q, J = 7.2 Hz, 2H), 1.29 (t, J = 7.2 Hz, 3H). ^{13}C NMR (100 MHz, $CDCl_3$): δ 171.13, 167.18, 161.59, 158.19, 140.25, 138.41, 137.30, 133.68, 133.22, 130.09, 129.82, 129.28, 128.89, 128.32, 128.22, 127.71, 127.31, 126.85, 119.73, 110.30, 60.98, 14.25. HRMS (ESI) calcd for: $C_{24}H_{20}N_2O_2S$ $[M+H]^+$ 401.1324, found 401.1318. Purity: 99% (method A, t_R = 10.81 min).

Ethyl 2-((3'-methoxy-[1,1'-biphenyl]-4-yl)amino)-4-phenylthiazole-5-carboxylate (50). mp 175.1-175.8 °C. ^{1}H NMR (400MHz, $CDCl_3$): δ 7.76-7.74 (m, 2H), 7.51 (d, J = 8.4 Hz, 2H), 7.41-7.37 (m, 4H), 7.17 (d, J = 8.4 Hz, 3H), 7.12 (d, J = 2.0 Hz, 1H), 6.93 (dd, J_1= 2.4 Hz, J_2 = 8.0 Hz, 1H), 4.28-4.22(q, J = 7.2 Hz, 2H), 3.91 (s, 3H), 1.28 (t, J = 7.2 Hz, 3H) .^{13}C NMR (100 MHz, $CDCl_3$): δ 167.62, 161.69, 160.01, 158.63, 141.82, 138.61, 137.09, 134.15, 129.88, 129.83, 129.16, 128.12, 127.71, 120.10, 119.35, 112.71, 112.52, 110.25, 60.91, 55.35, 14.26. HRMS (ESI) calcd for: $C_{25}H_{22}N_2O_3S$ $[M+H]^+$ 431.1429, found 431.1432. Purity: 95.7% (method A, t_R = 10.45 min).

Ethyl 2-((3-fluoro-[1,1'-biphenyl]-4-yl)amino)-4-phenylthiazole-5-carboxylate (51).

mp 175.1-177.0 °C. ^{1}H NMR (400MHz, $CDCl_3$): 7.98 (t, J = 8.4 Hz, 1H), 7.81-7.79 (m, 2H), 7.61-7.59(m, 2H), 7.50-7.40(m, 8H), 4.30-4.25(m, 2H), 1.30(t, J = 7.2 Hz, 3H). ^{13}C NMR (100 MHz, $CDCl_3$): 165.85, 161.61, 158.62, 154.64, 152.19, 139.25, 138.19, 138.11, 134.05, 129.75, 129.13, 129.01, 127.80, 127.60, 126.78, 126.72, 126.60, 123.25, 123.22, 120.69, 114.31, 114.11, 111.75, 61.04, 29.73, 14.24. HRMS (ESI) calcd for: $C_{24}H_{19}FN_2O_2S$ $[M+H]^+$ 419.1230,found 419.1232. Purity: 96.5% (method A, t_R = 11.33 min).

Ethyl 2-((3-fluoro-3'-methoxy-[1,1'-biphenyl]-4-yl)amino)-4-phenylthiazole-5-carboxylate (52). mp 166.6-166.8 °C.^{1}H NMR (400MHz, $CDCl_3$): δ 8.00 (t, J = 8.4 Hz, 1H), 7.82-7.79 (m, 2H), 7.48-7.38 (m, 6H), 7.18 (d, J = 7.6 Hz, 1H), 7.12 (s, 1H), 6.94 (dd, $J1$= 2.4 Hz, J_2= 8.4 Hz, 1H), 4.30-4.25 (m, 2H), 3.90 (s, 3H), 1.30 (t, J = 7.2 Hz, 3H). ^{13}C NMR (100 MHz, $CDCl_3$): δ 165.55, 161.57, 160.12, 158.54, 154.44, 152.00, 140.75, 137.92, 137.85, 134.05, 130.01, 129.77, 129.13, 127.60, 126.84, 126.73, 123.29, 123.26, 120.42, 119.25, 114.32, 114.12, 113.09, 112.64, 111.92, 61.03, 55.36, 14.21. HRMS (ESI) calcd for: $C_{25}H_{21}FN_2O_3S$ $[M+H]^+$ 449.1335, found 449.1331. Purity: 99.4% (method A, t_R = 10.96 min).

Ethyl 2-((3,5-difluoro-3'-methoxy-[1,1'-biphenyl]-4-yl)amino)-4-phenylthiazole-5-carboxylate (53). mp 197.9-198.6 °C. ^{1}H NMR (400MHz, $CDCl_3$): δ 7.66 (d, J = 7.6 Hz, 2H), 7.43 (t, J = 8.0 Hz, 1H), 7.26 (d, J = 7.0 Hz, 3H), 7.19-7.16 (m, 3H), 7.10 (s, 1H), 7.01 (d, J = 8.0 Hz, 1H), 4.22-4.17 (m, 2H), 3.92 (s, 3H), 1.22 (t, J = 7.2 Hz, 3H). ^{13}C NMR (100 MHz, $CDCl_3$): δ 170.93, 161.38, 160.18, 159.47, 159.43, 158.14, 156.97, 156.92, 141.94, 139.74, 133.57, 133.37, 130.25, 130.12, 129.49, 128.93, 128.36, 127.38, 119.30, 115.41, 113.95, 112.76, 111.48, 110.96, 110.72, 60.89, 55.43, 29.72, 14.18. HRMS (ESI) calcd for: $C_{25}H_{20}F_2N_2O_3S$ $[M+H]^+$ 467.1241, found 467.1235. Purity: 99.1% (method A, t_R = 9.51 min).

Ethyl 2-((3-chloro-4-phenoxyphenyl)amino)-4-phenylthiazole-5-carboxylate (54). mp 160.4-160.6 °C. ^{1}H NMR (400MHz, $CDCl_3$): δ 7.72 (s, 2H), 7.40-7.31 (m, 6H), 7.15 (t, J = 7.2 Hz, 1H), 7.07-7.05 (m, 1H), 6.99 (d, J = 7.6 Hz, 2H), 6.93 (d, J = 8.8 Hz, 1H), 4.27-4.22 (m, 2H), 1.27 (t, J = 7.2 Hz, 3H). ^{13}C NMR (100 MHz, $CDCl_3$): δ 168.09, 161.52, 158.51, 157.03, 149.29, 135.91, 133.93, 129.81, 129.66, 129.19, 127.70, 126.70, 123.41, 123.07, 121.57, 120.40, 117.68, 110.70, 60.96, 14.19. HRMS (ESI) calcd for: $C_{24}H_{19}ClN_2O_3S$ $[M+H]^+$ 451.0883, found 451.0882. Purity: 95.4% (method A, t_R =

11.24 min).

Ethyl 2-((4-(benzyloxy)-3-chlorophenyl)amino)-4-phenylthiazole-5-carboxylate (55). mp 165.9-166.6 °C. ^{1}H NMR (400MHz, $CDCl_3$): δ 7.70 (d, J = 3.2 Hz, 2H), 7.50 (d, J = 7.6 Hz, 2H), 7.44 (t, J = 8.8 Hz, 2H), 7.39-7.36 (m, 4H), 7.30 (d, J = 2.4 Hz, 1H), 7.09 (dd, J_1= 2.4 Hz, J_2= 8.8 Hz, 1H), 6.93 (d, J = 8.8 Hz, 1H), 5.20 (s, 2H), 4.25-4.20 (m, 2H), 1.26 (t, J = 7.2 Hz, 3H). ^{13}C NMR (100 MHz, $CDCl_3$): δ 169.48, 161.58, 158.70, 151.90, 136.39, 133.97, 133.30, 129.52, 129.03, 128.68, 128.15, 127.59, 127.12, 124.33, 124.00, 121.36, 114.76, 110.10, 77.35, 60.82, 14.19. HRMS (ESI) calcd for: $C_{25}H_{21}ClN_2O_3S$ $[M+H]^+$ 465.1040, found 465.1032. Purity: 99.7% (method A, t_R = 10.92 min).

Ethyl 2-((3-chloro-4-((2-chloro-6-fluorobenzyl)oxy)phenyl)amino)-4-phenylthiazole-5-carboxylate (56). mp 167.8-168.2 °C. ^{1}H NMR (400MHz, $CDCl_3$): δ 7.63-7.61 (m, 2H), 7.37-7.32 (m, 2H), 7.30-7.26 (m, 3H), 7.10 (t, J = 8.0 Hz, 1H), 7.01 (d, J = 2.4 Hz, 1H), 6.96 (d, J = 8.8 Hz, 1H), 6.90 (dd, J_1= 2.4 Hz, J_2= 8.8 Hz, 1H), 5.25 (s, 2H), 4.21 (q, J = 7.2 Hz, 2H), 1.24 (t, J = 7.2 Hz, 3H). ^{13}C NMR (100 MHz, $CDCl_3$): δ 169.36, 163.32, 161.62, 160.81, 158.77, 151.79, 136.72, 136.68, 133.91, 133.82, 131.07, 130.97, 129.53, 129.10, 127.63, 125.70, 125.67, 124.61, 124.14, 121.98, 121.81, 121.20, 115.65, 114.51, 114.28, 109.99, 62.96, 62.92, 60.86, 14.22. HRMS (ESI) calcd for: $C_{25}H_{19}Cl_2FN_2O_3S$ $[M+H]^+$ 517.0556, found 517.0562. Purity: 99.0% (method A, t_R = 9.95 min).

ASSOCIATED CONTENT

Supporting Information.

The docking scores of the compounds and *Hs*DHODH by Glide. This material is available free of charge via the Internet at http://pubs.acs.org.

Accession Code

The coordinate and structure factor files for *Hs*DHODH complex with compounds **12** and **33** are 4JGD and 4RLI.

AUTHOR INFORMATION

Corresponding Author

*For L.Z.: phone, +86-21-64250213; E-mail, zhulfl@ecust.edu.cn

*For X.Q.: phone, +86-21- 64251399; E-mail, xhqian@ecust.edu.cn

*For H.L.: Phone: +86-21-64250213; Email: hlli@ecust.edu.cn

Author Contributions

J.Z., L.H. and Y.D. performed research and drafted the manuscript; X.R., M.X., L.X., S.L and D.D. performed research and helped to draft the manuscript; J.H., Z.Z, R.W.

and L.Z. contributed materials and participated in the discussion of the results; X.L. interpreted data and drafted the manuscript; Y.X., X.Q. and H.L. designed and performed research, interpreted data and approved the final manuscript.

†These authors contributed equally.

Notes

The authors declare no competing financial interest.

ACKNOWLEDGMENTS

We thank the staff at Shanghai Synchrotron Radiation Facility for assistances with data collection. This work was supported by the Fundamental Research Funds for the Central Universities to Y.X., the National Natural Science Foundation of China (grants 81102375, 21372078, 81302697, 81222046 and 81230076) (X.L., Z.Z., L.Z., H.L.), the Shanghai Committee of Science and Technology (grant 14431902400) (H.L.), and the 863 Hi-Tech Program of China (grant 2012AA020308) (H.L.). Lili Zhu is also sponsored by the Shanghai Natural Science Fund for Youth Scholars (grant 12ZR144280). Honglin Li is also sponsored by Shanghai Rising-Star Tracking Program (grant 13QH1401100), the Innovation Program of Shanghai Municipal Education Commission (grant 13SG32) and Fok Ying Tung Education Foundation (141035).

Figure Captions

Figure1. Structure of known *Hs*DHODH inhibitors **1** leflunomide, **2** teriflunomide (A77 1726), **3** brequinar and lead compound **4** used in this study.

Figure 2. (A) Overall structure of *Hs*DHODH in complex with compound **12**. The structure is shown in cartoon and surface representation as generated by PyMOL (www.pymol.org). Compound **12** is presented in sphere model (B) Binding mode of compound **12** with *Hs*DHODH revealed by X–ray crystallography. 2*Fo*-*Fc* electron density is contoured at 1σ. The hydrogen bonds between are presented as black dashed lines. The water molecule is depicted as a red ball.

Figure 3. (A) The ubiquinone-binding pocket of *Hs*DHODH with compound **12** and **33** (PDB ID: 4JGD and 4RLI). The hydrophilic pockets are indicated with red dashed lines, and the hydrophobic cavities are highlighted by white dashed lines. The water molecules in 4JGD are depicted as red balls (B) The proposed binding pose of compound **47** against *Hs*DHODH via Induced Fit Docking method. The critical residues of the co-crystal structure of **12** and the docking mode of **47** are colored green and blue respectively, and the substrate FMN is presented as gray sticks. Hydrogen bonds are shown as yellow dashed lines.

Figure 4. Alignment of *Pf*DHODH (magenta, PDB code: 3I65) and the crystal structure

of *Hs*DHODH (cyan) in complex with compound **12**. The inhibitor is depicted as spheres, and the substrate FMN is presented as sticks. The non-conserved residues discussed in the text are shown as lines and labeled.

Figure 5. In vivo effects of compound **44** on collagen-induced arthritis in rats. Wistar rats were immunized on day 0 and day 7 with bovine type II collagen emulsified with an equal volume of incomplete Freund's adjuvant. Compound **44** (5 mg/kg and 30 mg/kg) and Methotrexate (0.3 mg/kg) were i.p. administered for 28 days. (A) The curves of body weight in different goups. (B) Arthritis scores in different treatments. (C) The representative photos of hind legs in different treatments on day 28. (D) Hematoxylin and Eosin staining of joint tissues in normal, CIA, compound **44** and methotrexate treated rats. S, synovium; C, cartilage; Bn, bone. Magnification = 50×. Data was expressed as mean ± SEM. $^{\#\#}$ $P < 0.01$ vs normal control, * $P < 0.05$, ** $P < 0.01$ vs CIA group.

Scheme 1. Synthetic Strategy for Thiazole-derived Compounds **4-56**

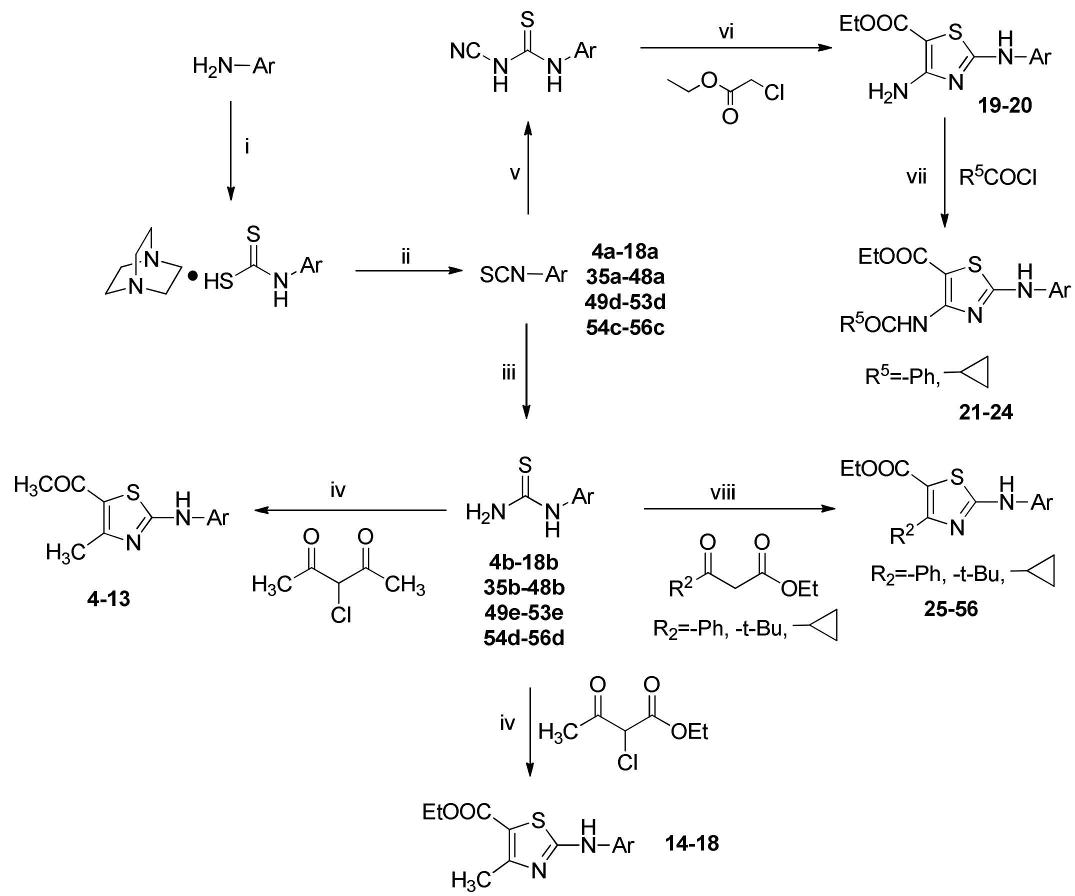

General conditions: (i) CS_2, triethylenediamine, Acetone, overnight at RT; (ii) triphosgene, Chloroform, overnight at RT; (iii) $NH_3\cdot H_2O$, Dichloromethane, 0 ^oC, 2-4 h; (iv) Methanol, reflux, overnight; (v) NaOEt/EtOH, cyanamide, overnight at RT; (**vi**) NaOEt/EtOH, overnight at, RT; (**vii**) triethylenediamine, Toluene, 90 ^oC; (**viii**) β-Cyclodextrin, NBS, H_2O/Acetone, 60 ^oC, (16-24) h.

Scheme 2. Synthesis of Aryl Amine Precursors **49c-53c**

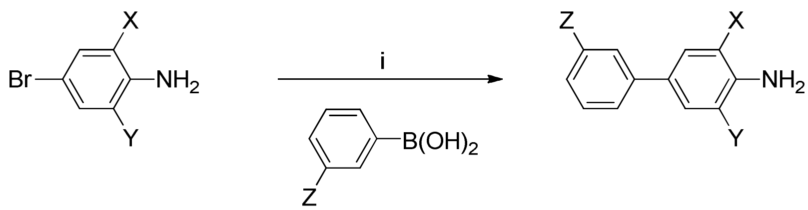

49a X=H,Y=H	**49b** Z=H	**49c** X=H, Y=H, Z=H
50a X=H, Y=H	**50b** Z=OCH_3	**50c** X=H, Y=H, Z=OCH_3
51a X=F, Y=H	**51b** Z=H	**51c** X=F, Y=H, Z=H
52a X=F,Y=H	**52b** Z=OCH_3	**52c** X=F, Y=H,Z=OCH_3
53a X=F,Y=F	**53b** Z=OCH_3	**53c** X=F, Y=F,Z=OCH_3

General conditions: (i) appropriate phenylboronic acid, $Pd(PPh_3)_4$, K_2CO_3, H_2O/EtOH/Benzene, reflux, overnight.

Scheme 3. Synthesis of Aryl Amine Precursors **54b-56b**

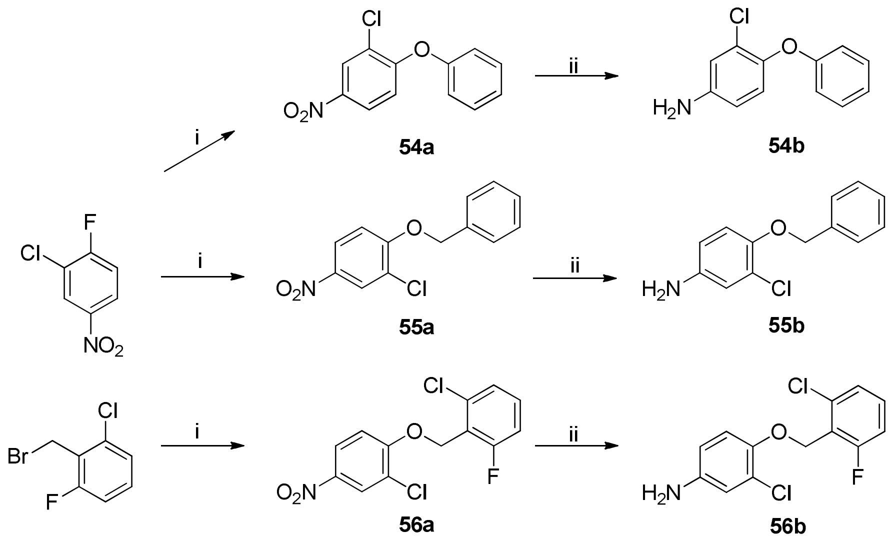

General conditions: (i) requisite aromatic alcohol or phenol, KOH, Acetonitrile, 40 °C, overnight; (ii) Fe, NH_4Cl, $EtOH/H_2O$, reflux, 0.5 h.

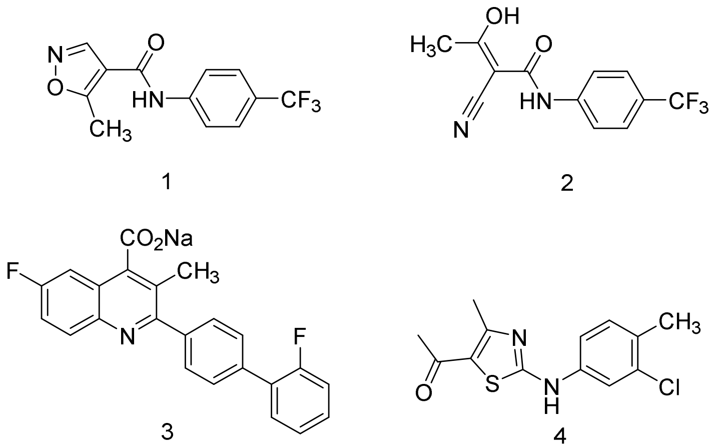

Figure 1. Structure of known *Hs*DHODH inhibitors **1** leflunomide, **2** teriflunomide (A77 1726), **3** brequinar and lead compound **4** used in this study

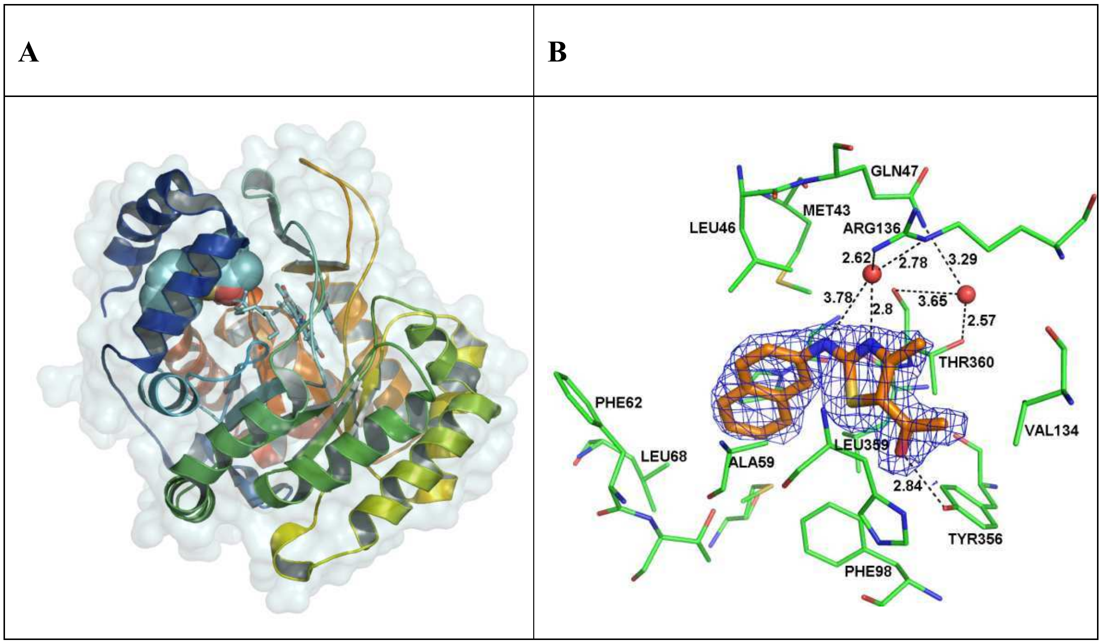

Figure 2. (A) Overall structure of *Hs*DHODH in complex with compound **12**. The structure is shown in cartoon and surface representation as generated by PyMOL (www.pymol.org). Compound **12** is presented in sphere model (B) Binding mode of compound **12** with *Hs*DHODH revealed by X-ray crystallography. 2*Fo*-*Fc* electron density is contoured at 1σ. The hydrogen bonds between are presented as black dashed lines. The water molecule is depicted as a red ball.

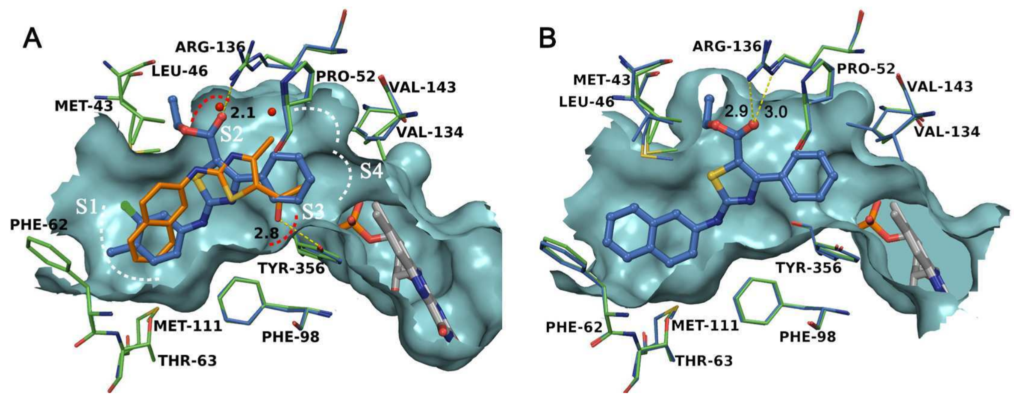

Figure 3. (A) The ubiquinone-binding pocket of *Hs*DHODH with compound **12** and **33** (PDB ID: 4JGD and 4RLI). The hydrophilic pockets are indicated with red dashed lines, and the hydrophobic cavities are highlighted by white dashed lines. The water molecules in 4JGD are depicted as red balls (B) The proposed binding pose of compound **47** against *Hs*DHODH via Induced Fit Docking method. The critical residues of the co-crystal structure of **12** and the docking mode of **47** are colored green and blue respectively, and the substrate FMN is presented as gray sticks. Hydrogen bonds are shown as yellow dashed lines.

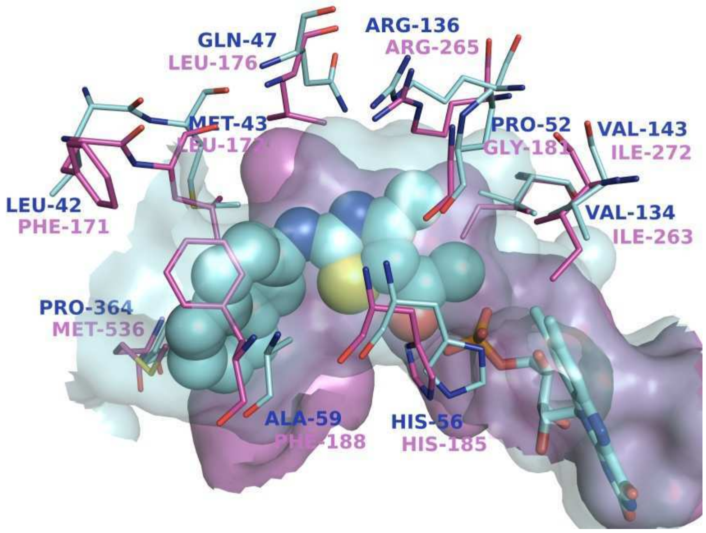

Figure 4. Alignment of *Pf*DHODH (magenta, PDB code: 3I65) and the crystal structure of *Hs*DHODH (cyan) in complex with compound **12**. The inhibitor is depicted as spheres, and the substrate FMN is presented as sticks. The non-conserved residues discussed in the text are shown as lines and labeled.

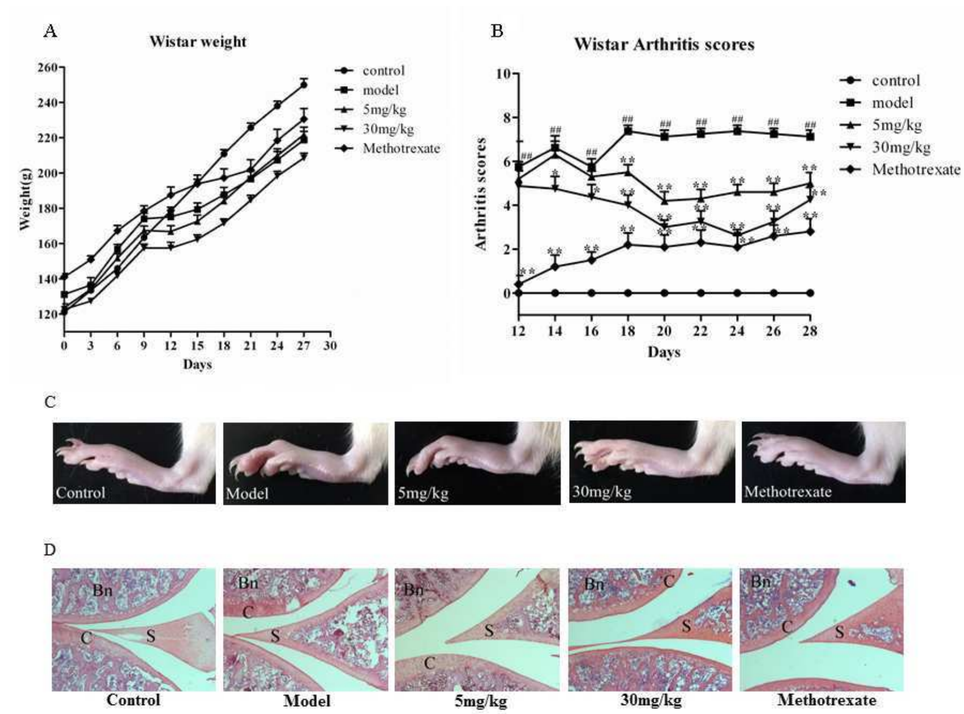

Figure 5. In vivo effects of compound **44** on collagen-induced arthritis in rats. Wistar rats were immunized on day 0 and day 7 with bovine type II collagen emulsified with an equal volume of incomplete Freund's adjuvant. Compound **44** (5 mg/kg and 30 mg/kg) and Methotrexate (0.3 mg/kg) were i.p. administered for 28 days. (A) The curves of body weight in different goups. (B) Arthritis scores in different treatments. (C) The representative photos of hind legs in different treatments on day 28. (D) Hematoxylin and Eosin staining of joint tissues in normal, CIA, compound **44** and methotrexate treated rats. S, synovium; C, cartilage; Bn, bone. Magnification = 50×. Data was expressed as mean ± SEM. ## $P < 0.01$ vs normal control, * $P < 0.05$, ** $P < 0.01$ vs CIA group.

Table 1. Structure-Activity Relationship (SAR) of 1-(4-methyl-2-(phenylamino)thiazol-5-yl)ethan-1-one derivatives 4-13

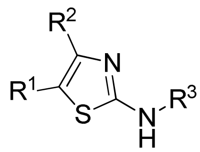

Compd	R^1	R^2	R^3	pKa[c]	logP[d]	logS[e]	IC$_{50}$(μM)	
							*Hs*DHODH[a]	*Pf*DHODH[b]
4	-COCH$_3$	-CH$_3$	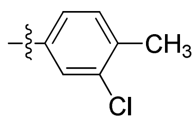	1.6	4.24	-3.59	3.937±0.169	0.630±0.028
5	-COCH$_3$	-CH$_3$	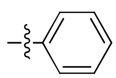	1.8	3.25	-2.56	>10	>10
6	-COCH$_3$	-CH$_3$	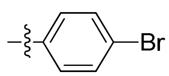	1.7	3.94	-3.42	>10	>10
7	-COCH$_3$	-CH$_3$	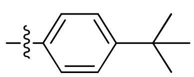	2.1	4.92	-4.23	3.649±0.495	>10
8	-COCH$_3$	-CH$_3$	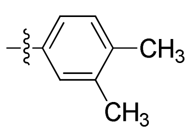	2.3	3.98	-3.26	3.848±0.110	1.489±0.015
9	-COCH$_3$	-CH$_3$	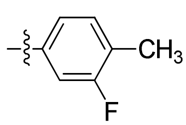	1.6	3.71	-3.25	>10	>10
10	-COCH$_3$	-CH$_3$	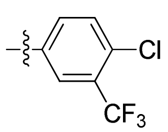	0.4	4.76	-3.97	2.346±0.006	4.265±0.572

11	-$COCH_3$	-CH_3	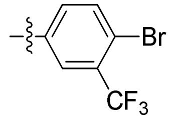	0.5	4.82	-4.15	1.926±0.029	>10
12	-$COCH_3$	-CH_3	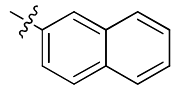	1.5	4.50	-3.94	0.562±0.005	0.871±0.020
13	-$COCH_3$	-CH_3	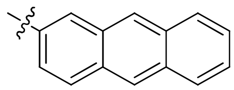	1.2	5.75	-5.33	>10	>10
A77 1726	--	--	--	11.5	2.38	-2.07	0.163±0.002	--
DSM1	--	--	--	3.0	3.62	-2.86	--	0.025±0.001

[a] The IC_{50} values of the compounds against *Hs*DHODH, in vitro assay, μM

[b] The IC_{50} values of the compounds against *Pf*DHODH, in vitro assay, μM

[c] Calculated using Jaguar pKa prediction module[44]

[d] Calculated using XLOGP3[45]

[e] Calculated using XLOGS[46]

Table 2. Data collection and refinement statistics for the *Hs*DHODH co-crystal structures

Inhibitor	**12**	**33**
Wavelengths (Å)	0.97852	0.97852
Space group	P 3_2 2 1	P 3_2 2 1
Cell dimensions (Å)	90.760/90.760/123.490	90.810/90.810/123.480
Resolution (Å)	48.55-2.05	48.56-2.50
Number of reflections	35529	19833
Redundancy	7.5(7.6)	8.4(8.4)
Completeness (%)	99.8(99.7)	100.0(100.0)
R_{merge} (%)	12.8(33.8)	13.0(33.5)
I/σ (I)	12.4(6.7)	13.4(6.4)
R/R_{free} (%)	16.0/17.5	17.8/21.2
Bonds(Å)	0.009	0.019
Angles (deg.)	1.741	2.056
PDB ID code	4JGD	4RLI

Table 3. Structure-Activity Relationship (SAR) of 15-33 by modification on R[1] and R[2]

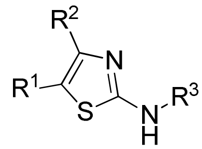

Compd	R[1]	R[2]	R[3]	pKa[c]	logP[d]	logS[e]	IC50(μM)	
							*Hs*DHODH[a]	*Pf*DHODH[b]
14	-COOEt	-CH_3	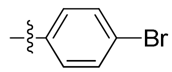	1.2	4.47	-4.07	9.074±0.953	2.452±0.493
15	-COOEt	-CH_3	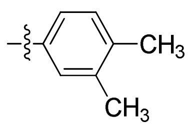	3.7	4.51	-3.91	1.358±0.036	>10
16	-COOEt	-CH_3	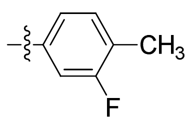	2	4.25	-3.90	1.987±0.001	>10
17	-COOEt	-CH_3	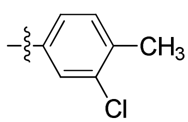	2.9	4.77	-4.23	0.969±0.012	>10
18	-COOEt	-CH_3	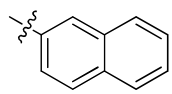	2.8	5.03	-4.59	0.887±0.058	>10
19	-COOEt	-NH_2	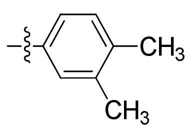	1.5	4.31	-3.89	2.111±0.018	>10
20	-COOEt	-NH_2	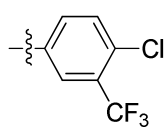	3.5	5.10	-4.59	>10	>10
21	-COOEt	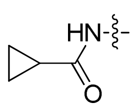	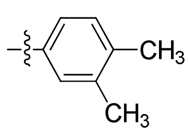	2.6	4.63	-4.48	>10	>10

22	-COOEt	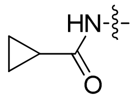	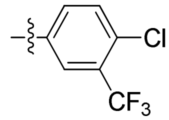	1	5.41	-5.18	6.040±0.084	>10
23	-COOEt	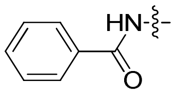	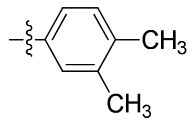	2.1	5.83	-5.38	9.028±3.480	>10
24	-COOEt	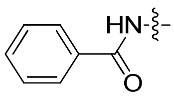	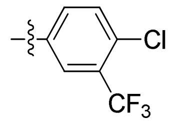	0.7	6.61	-6.09	>10	>10
25	-COOEt	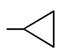	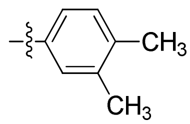	0.3	4.69	-4.19	0.325±0.008	>10
26	-COOEt	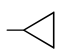	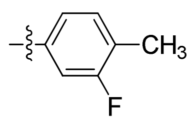	0.2	4.42	-4.18	0.645±0.002	>10
27	-COOEt	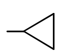	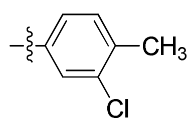	0.2	4.95	-4.51	0.372±0.026	>10
28	-COOEt	-t-Bu	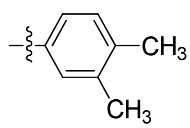	3.1	5.82	-5.22	0.515±0.008	>10
29	-COOEt	-t-Bu	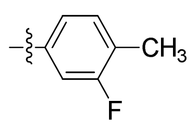	2.4	5.55	-5.21	0.652±0.003	>10
30	-COOEt	-t-Bu	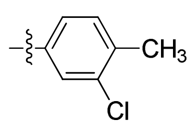	2.5	6.08	-5.55	0.552±0.019	>10
31	-COOEt	-Ph	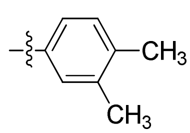	2	5.77	-5.22	0.058±0.001	>10

32	-COOEt	-Ph	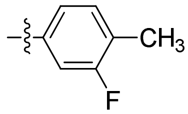	1.5 [1.44±0.98]	5.51	-5.21 [<-4.30]	0.049±0.004	>10
33	-COOEt	-Ph	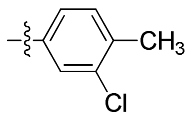	1.3 [1.85±1.11]	6.04	-5.54 [<-4.30]	0.035±0.004	>10

[a] The IC_{50} values of the compounds against *Hs*DHODH, in vitro assay, μM

[b] The IC_{50} values of the compounds against *Pf*DHODH, in vitro assay, μM

[c] Calculated using Jaguar pKa prediction module,[44] values in square brackets are measured using Sirius T3 Station.

[d] Calculated using XLOGP3[45]

[e] Calculated using XLOGS,[46] values in square brackets are measured using Sirius T3 Station.

Table 4. Further Structure-Activity Relationship (SAR) of 34-56 by modification on R^3

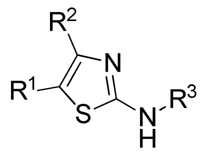

Compd	R^1	R^2	R^3	pKa[c]	logP[d]	logS[e]	IC_{50}(μM)	
							*Hs*DHODH[a]	*Pf*DHODH[b]
34	-COOEt	-Ph	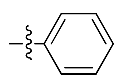	1.6	5.04	-4.52	0.784±0.016	>10
35	-COOEt	-Ph	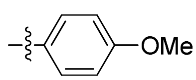	2.2	5.01	-4.65	1.440±0.512	>10
36	-COOEt	-Ph	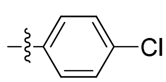	1.3	5.67	-5.19	0.239±0.007	>10
37	-COOEt	-Ph	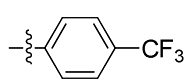	0.5	5.93	-5.25	0.408±0.015	>10
38	-COOEt	-Ph	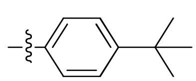	2	6.71	-6.18	0.284±0.012	>10
39	-COOEt	-Ph	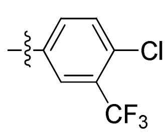	0.5	6.56	-5.93	0.131±0.001	>10
40	-COOEt	-Ph	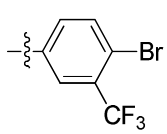	0.5	6.62	-6.11	0.128±0.018	>10

41	-COOEt	-Ph	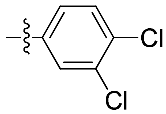	1	6.30	-5.87	0.174±0.014	>10
42	-COOEt	-Ph	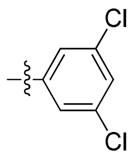	0.5	6.30	-5.87	0.393±0.006	>10
43	-COOEt	-Ph	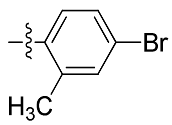	0.7	6.10	-5.72	>10	>10
44	-COOEt	-Ph	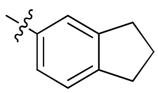	2.1 [1.35±0.01]	5.88	-5.46 [<-4.30]	0.026±0.005	>10
45	-COOEt	-Ph	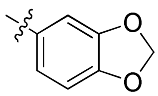	2.3	4.86	-4.96	1.108±0.143	>10
46	-COOEt	-Ph	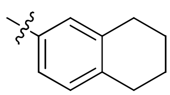	2.1	6.42	-5.85	0.018±0.005	>10
47[f]	-COOEt	-Ph	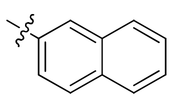	1.3 [1.51±0.56]	6.29	-5.90 [<-4.30]	0.029±0.002	>10
48	-COOEt	-Ph	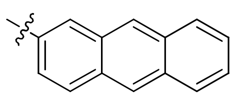	1.1	7.54	-7.28	0.453±0.022	>10
49	-COOEt	-Ph	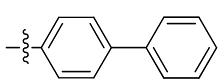	1.5	6.67	-6.18	>10	>10
50	-COOEt	-Ph	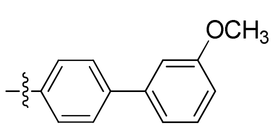	1.4	6.64	-6.31	>10	>10

51	-COOEt	-Ph	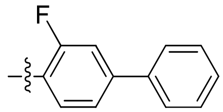	0.7	6.77	-6.52	>10	>10
52	-COOEt	-Ph	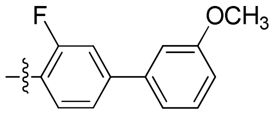	0.9	6.74	-6.65	>10	>10
53	-COOEt	-Ph	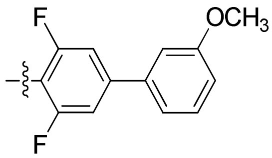	1.2	6.84	-6.99	0.311±0.019	>10
54	-COOEt	-Ph	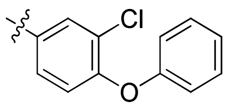	1.7	7.20	-6.77	>10	>10
55	-COOEt	-Ph	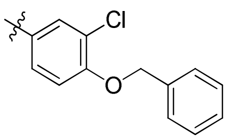	1.8	7.14	-6.85	>10	>10
56	-COOEt	-Ph	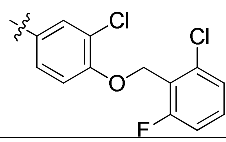	0.9	7.86	-7.87	>10	>10

[a] The IC_{50} values of the compounds against *Hs*DHODH, in vitro assay, μM

[b] The IC_{50} values of the compounds against *Pf*DHODH, in vitro assay, μM

[c] Calculated using Jaguar pKa prediction module,[44] values in square brackets are measured using Sirius T3 Station.

[d] Calculated using XLOGP3[45]

[e] Calculated using XLOGS,[46] values in square brackets are measured using Sirius T3 Station.

[f] Compounds commercially obtained.

REFERENCES

(1) Löffler, M.; Fairbanks, L. D.; Zameitat, E.; Marinaki, A. M.; Simmonds, H. A. Pyrimidine pathways in health and disease. *Trends Mol. Med.* **2005**, *11* (9), 430-437.

(2) Munier-Lehmann, H.; Vidalain, P.-O.; Tangy, F.; Janin, Y. L. On Dihydroorotate Dehydrogenases and Their Inhibitors and Uses. *J. Med. Chem.* **2013**, *56* (8), 3148-3167.

(3) Vyas, V. K.; Ghate, M. Recent developments in the medicinal chemistry and therapeutic potential of dihydroorotate dehydrogenase (DHODH) inhibitors. *Mini Rev. Med. Chem.* **2011**, *11* (12), 1039-1055.

(4) Nørager, S.; Jensen, K. F.; Björnberg, O.; Larsen, S. E. coli Dihydroorotate Dehydrogenase Reveals Structural and Functional Distinctions between Different Classes of Dihydroorotate Dehydrogenases. *Structure* **2002**, *10* (9), 1211-1223.

(5) Krungkrai, J. Purification, characterization and localization of mitochondrial dihydroorotate dehydrogenase in Plasmodium falciparum, human malaria parasite. *Biochim. Biophys. Acta* **1995**, *1243* (3), 351-360.

(6) Hansen, M.; Le Nours, J.; Johansson, E.; Antal, T.; Ullrich, A.; Löffler, M.; Larsen, S. Inhibitor binding in a class 2 dihydroorotate dehydrogenase causes variations in the membrane-associated N-terminal domain. *Protein Sci.* **2004**, *13* (4), 1031-1042.

(7) Palfey, B. A.; Björnberg, O.; Jensen, K. F. Insight into the Chemistry of Flavin

Reduction and Oxidation in Escherichia coli Dihydroorotate Dehydrogenase Obtained by Rapid Reaction Studies†. *Biochemistry* **2001**, *40* (14), 4381-4390.

(8) Breedveld, F. C.; Dayer, J. M. Leflunomide: mode of action in the treatment of rheumatoid arthritis. *Ann. Rheum. Dis.* **2000**, *59* (11), 841-849.

(9) Baumann, P.; Mandl-Weber, S.; Völkl, A.; Adam, C.; Bumeder, I.; Oduncu, F.; Schmidmaier, R. Dihydroorotate dehydrogenase inhibitor A771726 (leflunomide) induces apoptosis and diminishes proliferation of multiple myeloma cells. *Mol. Cancer Ther.* **2009**, *8* (2), 366-375.

(10) Chen, S.-F.; Ruben, R. L.; Dexter, D. L. Mechanism of Action of the Novel Anticancer Agent 6-Fluoro-2-(2′-fluoro-1,1′-biphenyl-4-yl)-3-methyl-4-quinolinecarboxylic Acid Sodium Salt (NSC 368390): Inhibition of de Novo Pyrimidine Nucleotide Biosynthesis. *Cancer Res.* **1986**, *46* (10), 5014-5019.

(11) Merrill, J.; Hanak, S.; Pu, S.-F.; Liang, J.; Dang, C.; Iglesias-Bregna, D.; Harvey, B.; Zhu, B.; McMonagle-Strucko, K. Teriflunomide reduces behavioral, electrophysiological, and histopathological deficits in the Dark Agouti rat model of experimental autoimmune encephalomyelitis. *J. Neurol.* **2009**, *256* (1), 89-103.

(12) Herrmann, M. L.; Schleyerbach, R.; Kirschbaum, B. J. Leflunomide: an

immunomodulatory drug for the treatment of rheumatoid arthritis and other autoimmune diseases. *Immunopharmacology* **2000**, *47* (2-3), 273-289.

(13) Fox, R. I.; Herrmann, M. L.; Frangou, C. G.; Wahl, G. M.; Morris, R. E.; Strand, V.; Kirschbaum, B. J. Mechanism of Action for Leflunomide in Rheumatoid Arthritis. *Clin. Immunol.* **1999**, *93* (3), 198-208.

(14) Alldred, A.; Emery, P. Leflunomide: a novel DMARD for the treatment of rheumatoid arthritis. *Expert Opin. Pharmacother.* **2001**, *2* (1), 125-137.

(15) Cramer, D. V.; Chapman, F. A.; Jaffee, B. D.; Jones, E. A.; Knoop, M.; Hreha-Eiras, G.; Makowka, L. The effect of a new immunosuppressive drug, brequinar sodium, on heart, liver, and kidney allograft rejection in the rat. *Transplantation* **1992**, *53* (2), 303-308.

(16) Cohen, S.; Cannon, G. W.; Schiff, M.; Weaver, A.; Fox, R.; Olsen, N.; Furst, D.; Sharp, J.; Moreland, L.; Caldwell, J.; Kaine, J.; Strand, V. Two-year, blinded, randomized, controlled trial of treatment of active rheumatoid arthritis with leflunomide compared with methotrexate. *Arthritis Rheum.* **2001**, *44* (9), 1984-1992.

(17) Emery, P.; Breedveld, F. C.; Lemmel, E. M.; Kaltwasser, J. P.; Dawes, P. T.; Gömör, B.; Van den Bosch, F.; Nordström, D.; Bjørneboe, O.; Dahl, R.; Hørslev - Petersen, K.; Rodriguez de la Serna, A.; Molloy, M.; Tikly, M.; Oed, C.; Rosenburg, R.;

Loew‐Friedrich, I.; Group, t. M. L. S. A comparison of the efficacy and safety of leflunomide and methotrexate for the treatment of rheumatoid arthritis. *Rheumatology (Oxford)* **2000**, *39* (6), 655-665.

(18) Jian, X.; Guo, G.; Ruan, Y.; Lin, D.; Li, X. Severe Cutaneous Adverse Drug Reaction to Leflunomide: A Report of Two Cases. *Cutan. Ocul. Toxicol.* **2008**, *27* (1), 5-9.

(19) Burris, H., III; Raymond, E.; Awada, A.; Kuhn, J.; O'Rourke, T.; Brentzel, J.; Lynch, W.; King, S.-Y.; Brown, T.; Von Hoff, D. Pharmacokinetic and phase I studies of brequinar (DUP 785; NSC 368390) in combination with cisplatin in patients with advanced malignancies. *Invest. New Drugs* **1998**, *16* (1), 19-27.

(20) Makowka, L.; Tixier, D.; Chaux, A.; Hill, D.; O'Neill, P.; Eiras-Hreha, G.; Wu, G. D.; Cunneen, S.; Cajulis, E.; Zajac, I.; et al. Use of brequinar sodium for preventing cardiac allograft rejection in primates. *Transplant. Proc.* **1993**, *25* (3 Suppl 2), 48-53.

(21) Pally, C.; Smith, D.; Jaffee, B.; Magolda, R.; Zehender, H.; Dorobek, B.; Donatsch, P.; Papageorgiou, C.; Schuurman, H. J. Side effects of brequinar and brequinar analogues, in combination with cyclosporine, in the rat. *Toxicology* **1998**, *127* (1-3), 207-222.

(22) Kulkarni, O. P.; Sayyed, S. G.; Kantner, C.; Ryu, M.; Schnurr, M.; Sardy, M.;

Leban, J.; Jankowsky, R.; Ammendola, A.; Doblhofer, R.; Anders, H. J. 4SC-101, a novel small molecule dihydroorotate dehydrogenase inhibitor, suppresses systemic lupus erythematosus in MRL-(Fas)lpr mice. *Am. J. Pathol.* **2010**, *176* (6), 2840-2847.

(23) Walse, B.; Dufe, V. T.; Svensson, B.; Fritzson, I.; Dahlberg, L.; Khairoullina, A.; Wellmar, U.; Al-Karadaghi, S. The structures of human dihydroorotate dehydrogenase with and without inhibitor reveal conformational flexibility in the inhibitor and substrate binding sites. *Biochemistry* **2008**, *47* (34), 8929-8936.

(24) Erra, M.; Moreno, I.; Sanahuja, J.; Andres, M.; Reinoso, R. F.; Lozoya, E.; Pizcueta, P.; Godessart, N.; Castro-Palomino, J. C. Biaryl analogues of teriflunomide as potent DHODH inhibitors. *Bioorg. Med. Chem. Lett.* **2011**, *21* (24), 7268-7272.

(25) Hurt, D. E.; Sutton, A. E.; Clardy, J. Brequinar derivatives and species-specific drug design for dihydroorotate dehydrogenase. *Bioorg. Med. Chem. Lett.* **2006**, *16* (6), 1610-1615.

(26) White, R. M.; Cech, J.; Ratanasirintrawoot, S.; Lin, C. Y.; Rahl, P. B.; Burke, C. J.; Langdon, E.; Tomlinson, M. L.; Mosher, J.; Kaufman, C.; Chen, F.; Long, H. K.; Kramer, M.; Datta, S.; Neuberg, D.; Granter, S.; Young, R. A.; Morrison, S.; Wheeler, G. N.; Zon, L. I. DHODH modulates transcriptional elongation in the neural crest and melanoma. *Nature* **2011**, *471* (7339), 518-522.

(27) Wang, Q. Y.; Bushell, S.; Qing, M.; Xu, H. Y.; Bonavia, A.; Nunes, S.; Zhou, J.; Poh, M. K.; de Sessions, P. F.; Niyomrattanakit, P.; Dong, H. P.; Hoffmaster, K.; Goh, A.; Nilar, S.; Schul, W.; Jones, S.; Kramer, L.; Compton, T.; Shi, P. Y. Inhibition of Dengue Virus through Suppression of Host Pyrimidine Biosynthesis. *J. Virol.* **2011**, *85* (13), 6548-6556.

(28) Leban, J.; Kralik, M.; Mies, J.; Gassen, M.; Tentschert, K.; Baumgartner, R. SAR, species specificity, and cellular activity of cyclopentene dicarboxylic acid amides as DHODH inhibitors. *Bioorg. Med. Chem. Lett.* **2005**, *15* (21), 4854-4857.

(29) Leban, J.; Kralik, M.; Mies, J.; Baumgartner, R.; Gassen, M.; Tasler, S. Biphenyl-4-ylcarbamoyl thiophene carboxylic acids as potent DHODH inhibitors. *Bioorg. Med. Chem. Lett.* **2006**, *16* (2), 267-270.

(30) Kim, T. H.; Na, H. S.; Loffler, M. Synthesis of beta-hydroxy-propenamide derivatives and the inhibition of human dihydroorotate dehydrogenase. *Arch. Pharm. Res.* **2003**, *26* (3), 197-201.

(31) Diao, Y.; Lu, W.; Jin, H.; Zhu, J.; Han, L.; Xu, M.; Gao, R.; Shen, X.; Zhao, Z.; Liu, X.; Xu, Y.; Huang, J.; Li, H. Discovery of Diverse Human Dihydroorotate Dehydrogenase Inhibitors as Immunosuppressive Agents by Structure-Based Virtual Screening. *J. Med. Chem.* **2012**, *55* (19), 8341-8349.

(32) Goodyer, C. L. M.; Chinje, E. C.; Jaffar, M.; Stratford, I. J.; Threadgill, M. D. Synthesis of N-benzyl- and N-phenyl-2-amino-4,5-dihydrothiazoles and thioureas and evaluation as modulators of the isoforms of nitric oxide synthase. *Biorg. Med. Chem.* **2003**, *11* (19), 4189-4206.

(33) Shi, H.-B.; Zhang, S.-J.; Ge, Q.-F.; Guo, D.-W.; Cai, C.-M.; Hu, W.-X. Synthesis and anticancer evaluation of thiazolyl–chalcones. *Bioorg. Med. Chem. Lett.* **2010**, *20* (22), 6555-6559.

(34) Yip, S. F.; Cheung, H. Y.; Zhou, Z.; Kwong, F. Y. Room-Temperature Copper-Catalyzed α-Arylation of Malonates. *Org. Lett.* **2007**, *9* (17), 3469-3472.

(35) Yang, Y.; Seidlits, S. K.; Adams, M. M.; Lynch, V. M.; Schmidt, C. E.; Anslyn, E. V.; Shear, J. B. A Highly Selective Low-Background Fluorescent Imaging Agent for Nitric Oxide. *J. Am. Chem. Soc.* **2010**, *132* (38), 13114-13116.

(36) Baumgartner, R.; Walloschek, M.; Kralik, M.; Gotschlich, A.; Tasler, S.; Mies, J.; Leban, J. Dual binding mode of a novel series of DHODH inhibitors. *J. Med. Chem.* **2006**, *49* (4), 1239-1247.

(37) Knecht, W.; Henseling, J.; Löffler, M. Kinetics of inhibition of human and rat dihydroorotate dehydrogenase by atovaquone, lawsone derivatives, brequinar sodium and polyporic acid. *Chem. Biol. Interact.* **2000**, *124* (1), 61-76.

(38) McLean, J. E.; Neidhardt, E. A.; Grossman, T. H.; Hedstrom, L. Multiple inhibitor analysis of the brequinar and leflunomide binding sites on human dihydroorotate dehydrogenase. *Biochemistry* **2001**, *40* (7), 2194-2200.

(39) Ullrich, A.; Knecht, W.; Fries, M.; Löffler, M. Recombinant expression of N-terminal truncated mutants of the membrane bound mouse, rat and human flavoenzyme dihydroorotate dehydrogenase. *Eur. J. Biochem.* **2001**, *268* (6), 1861-1868.

(40) Bedingfield, P. T. P.; Cowen, D.; Acklam, P.; Cunningham, F.; Parsons, M. R.; McConkey, G. A.; Fishwick, C. W. G.; Johnson, A. P. Factors Influencing the Specificity of Inhibitor Binding to the Human and Malaria Parasite Dihydroorotate Dehydrogenases. *J. Med. Chem.* **2012**, *55* (12), 5841-5850.

(41) Deng, X. Y.; Gujjar, R.; El Mazouni, F.; Kaminsky, W.; Malmquist, N. A.; Goldsmith, E. J.; Rathod, P. K.; Phillips, M. A. Structural Plasticity of Malaria Dihydroorotate Dehydrogenase Allows Selective Binding of Diverse Chemical Scaffolds. *J. Biol. Chem.* **2009**, *284* (39), 26999-27009.

(42) Hurt, D. E.; Widom, J.; Clardy, J. Structure of Plasmodium falciparum dihydroorotate dehydrogenase with a bound inhibitor. *Acta Crystallogr. D Biol. Crystallogr.* **2006**, *62* (3), 312-323.

(43) Xu, M.; Zhu, J.; Diao, Y.; Zhou, H.; Ren, X.; Sun, D.; Huang, J.; Han, D.;

Zhao, Z.; Zhu, L.; Xu, Y.; Li, H. Novel Selective and Potent Inhibitors of Malaria Parasite Dihydroorotate Dehydrogenase: Discovery and Optimization of Dihydrothiophenone Derivatives. *J. Med. Chem.* **2013**, *56* (20), 7911-7924.

(44) Jaguar, version 7.6; Schrödinger, Inc.: New York, 2009.

(45) Cheng, T. J.; Zhao, Y.; Li, X.; Lin, F.; Xu, Y.; Zhang, X. L.; Li, Y.; Wang, R. X.; Lai, L. H. Computation of octanol-water partition coefficients by guiding an additive model with knowledge. *J. Chem. Inf. Model.* **2007**, *47* (6), 2140-2148.

(46) Duan, B. G.; Li, Y.; Li, J.; Cheng, T. J.; Wang, R. X. An Empirical Additive Model for Aqueous Solubility Computation: Success and Limitations. *Acta Phys-Chim. Sin.* **2012**, *28* (10), 2249-2257.

(47) Liu, S.; Neidhardt, E. A.; Grossman, T. H.; Ocain, T.; Clardy, J. Structures of human dihydroorotate dehydrogenase in complex with antiproliferative agents. Structure **2000**, 8 (1), 25-33.

(48) Malmquist, N. A.; Baldwin, J.; Phillips, M. A. Detergent-dependent Kinetics of Truncated Plasmodium falciparumDihydroorotate Dehydrogenase. *J. Biol. Chem.* **2007**, *282* (17), 12678-12686.

(49) Powell, H. The Rossmann Fourier autoindexing algorithm in MOSFLM. *Acta Crystallogr. D Biol. Crystallogr.* **1999**, *55* (10), 1690-1695.

(50) The CCP4 suite: programs for protein crystallography. *Acta Crystallogr. D Biol. Crystallogr.* **1994**, *50* (Pt 5), 760-763.

(51) Potterton, E.; Briggs, P.; Turkenburg, M.; Dodson, E. A graphical user interface to the CCP4 program suite. *Acta Crystallogr. D Biol. Crystallogr.* **2003**, *59* (7), 1131-1137.

(52) Murshudov, G. N.; Vagin, A. A.; Dodson, E. J. Refinement of macromolecular structures by the maximum-likelihood method. *Acta Crystallogr. D Biol. Crystallogr.* **1997**, *53* (Pt 3), 240-255.

(53) Emsley, P.; Lohkamp, B.; Scott, W. G.; Cowtan, K. Features and development of Coot. *Acta Crystallogr. D Biol. Crystallogr.* **2010**, *66* (4), 486-501.

(54) Yue, R. C.; Zhao, L.; Hu, Y. H.; Jiang, P.; Wang, S. P.; Xiang, L.; Liu, W. C.; Zhang, W. D.; Liu, R. H. Rapid-resolution liquid chromatography TOF-MS for urine metabolomic analysis of collagen-induced arthritis in rats and its applications. *J. Ethnopharmacol.* **2013**, *145* (2), 465-475.

(55) Weinblatt, M. E. Methotrexate in rheumatoid arthritis: a quarter century of development. *Trans. Am. Clin. Climatol. Assoc.* **2013**, *124*, 16.

(56) Rosillo, M. A.; Alcaraz, M. J.; Sanchez-Hidalgo, M.; Fernandez-Bolanos, J. G.; Alarcon-de-la-Lastra, C.; Ferrandiz, M. L. Anti-inflammatory and joint protective

effects of extra-virgin olive-oil polyphenol extract in experimental arthritis. *J. Nutr. Biochem.* **2014**, *25*(12), 1275-1281.

TOC

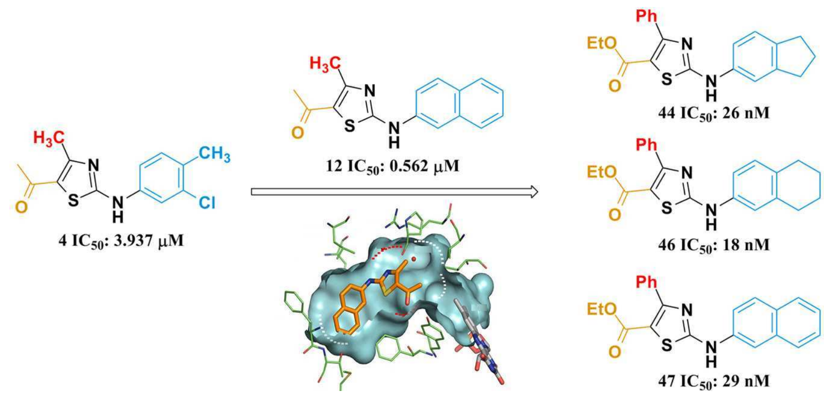
H3C
CH3
Cl
4 IC50: 3.937 μM
12 IC50: 0.562 μM
Ph
EtO
44 IC50: 26 nM
46 IC50: 18 nM
47 IC50: 29 nM